Volume 11 | Number 11 | 7 June 2024

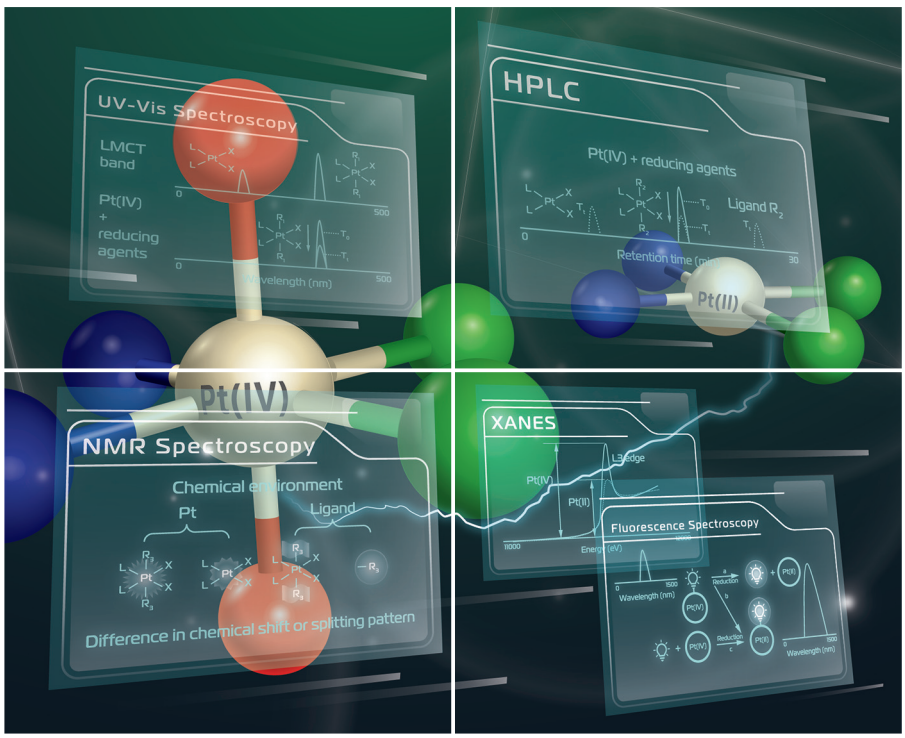

INORGANIC CHEMISTRY

FRONTIERS

CCS 中国化学会 CHINESE CHEMICAL SOCIETY
PEKING UNIVERSITY 1898
ROYAL SOCIETY OF CHEMISTRY
rsc.li/frontiers-inorganic

INORGANIC CHEMISTRY
FRONTIERS

REVIEW

View Article Online
View Journal | View Issue

Cite this: *Inorg. Chem. Front.*, 2024, **11**, 3085

Advances in technical strategies for monitoring the reduction of platinum(IV) complexes

Shu Chen,[a,b] Qiyuan Zhou,[a,b] Ka-Yan Ng,[a,b] Zoufeng Xu,[a,b] Weikang Xu[a] and Guangyu Zhu *[a,b]

Platinum(IV) prodrugs have emerged as highly promising candidates for next-generation anticancer drugs. The activation of these prodrugs heavily relies on the critical step of chemical reduction of platinum, which determines their ultimate efficacy as potent anticancer agents. Therefore, it is essential to employ effective strategies to monitor the reduction of Pt(IV) complexes and the generation of active Pt(II) counterparts. These strategies not only unravel the intracellular mechanisms but also facilitate the design of novel Pt(IV) prodrugs for cancer therapy and enable the prediction of their anticancer performance. In this review, we summarize recent advances in strategies used to monitor the reduction profiles of Pt(IV) complexes from an introductory yet comprehensive viewpoint. We first delve into the principles underlying the reduction of Pt(IV) prodrugs to Pt(II) species, with a focus on the detection foundations that rely on changes in molecular weight, electronic arrangement, and coordination patterns. We subsequently summarize the strategies employed to investigate the reduction progress of Pt(IV) complexes in both aqueous solutions and at the cellular level, while highlighting the scope of applications, advantages, and disadvantages of each method. Finally, we provide a concise summary and a critical assessment of the discussed approaches. We hope this account will empower researchers with a deeper understanding of the strategies for monitoring the activation of Pt(IV) prodrugs and shed light on the underlying mechanism of prodrug activation.

Received 20th February 2024,
Accepted 13th April 2024

DOI: 10.1039/d4qi00459k

rsc.li/frontiers-inorganic

1. Introduction

The discovery of cisplatin's antiproliferative properties by Rosenberg, through a serendipitous finding, marked a significant breakthrough in cancer treatment.[1–4] Cisplatin's successful application in treating metastatic ovarian and testicular

[a]*Department of Chemistry, City University of Hong Kong, Hong Kong SAR, P. R. China. E-mail: guangzhu@cityu.edu.hk*
[b]*City University of Hong Kong Shenzhen Research Institute, Shenzhen 518057, P. R. China*

Shu Chen

Shu Chen obtained her B.Sc. in Chemistry (2018) from Nanjing Normal University. She completed her Ph.D. at the City University of Hong Kong (2023) under the supervision of Prof. Guangyu Zhu. Her Ph.D. work centered on the design and synthesis of novel platinum(IV) anticancer prodrugs bearing different linkers and the exploration of activation of platinum(IV) prodrugs in live cells. Currently, she holds a postdoctoral position in Prof. Guangyu Zhu's research group.

Qiyuan Zhou

Qiyuan Zhou obtained his joint B.Sc. in Chemical Technology from Sun Yat-Sen University and the Hong Kong Polytechnic University (2018). He obtained an M.Sc. in chemistry from the City University of Hong Kong in 2019, and currently, he is a Ph. D. candidate at the same institute under the supervision of Prof. Guangyu Zhu. His research interests focus on the synthesis and development of novel Pt(II) and Pt(IV) anticancer agents.

cancers has led to significant improvements in the survival rates of numerous cancer patients.[5,6] This success spurred a further exploration into platinum-based anticancer agents, resulting in the development of carboplatin and oxaliplatin as second- and third-generation platinum-based drugs (Fig. 1A).[7–10] These drugs have become indispensable tools in the global fight against cancer.[11,12] Additionally, other Pt(II) drugs, such as nedaplatin, heptaplatin, lobaplatin, miriplatin, and dicycloplatin (Fig. 1B), have been approved for use in Japan (1995), Korea (1999), China (2003), Japan (2009), and China (2012), respectively, further expanding the armamentarium against cancer.[13]

The mechanism of action of Pt(II) drugs has been extensively explored.[5,11,14–16] Upon crossing the cell membrane, these drugs undergo aquation, a process that activates them. Subsequently, they bind to the N7 positions of guanine nucleobases in DNA, forming platinum-DNA adducts, which include both intra- and inter-strand crosslinks. These adducts distort the DNA structure, triggering a range of cellular responses that lead to cell cycle arrest and apoptosis, ultimately resulting in the death of cancer cells. While Pt(II) drugs have shown great promise in cancer treatment, their lack of inertness and selectivity has been associated with severe side effects during drug administration.[1,17,18] Moreover, tumor cells can develop resistance to these drugs, either as intrinsic properties of certain types of tumor cells or as a consequence of prolonged drug exposure.[1,19,20] These challenges present substantial obstacles to the effectiveness of Pt(II)-based antitumor therapy.

In recent years, significant progress has been made with the development of Pt(IV) prodrugs. These Pt(IV) complexes have emerged as alternative Pt-based drugs, aiming to minimize side effects, improve drug efficiency, and overcome drug resistance. Pt(IV) complexes possess a low-spin d^6 electronic configuration and an octahedral geometry with six coordinating ligands. This configuration reduces the likelihood of ligand exchange reactions, thus minimizing side effects.[21–23] Additionally, Pt(IV) prodrugs offer an advantage over Pt(II) counterparts by providing two additional axial ligands that can be tailored to improve drug efficiency and overcome drug resistance. It should be noted that in octahedral geometry, the terms "equatorial" and "axial" are not strictly defined. In order to differentiate, however, the intrinsic ligands of Pt(II) drugs are typically referred to as equatorial ligands, whereas the ligands introduced during the oxidation process are commonly called axial ligands. The incorporation of lipophilic moieties in Pt(IV) complexes promotes optimal cellular uptake,[24–26] while the inclusion of tumor-targeting agents enhances specificity for cancer cells,[27–30] thereby potentially amplifying the effectiveness of anticancer therapies. Moreover, upon reduction, the bioactive moieties initially integrated into Pt(IV) complexes can act synergically with released Pt(II) drugs, ultimately overcoming drug resistance.[31–34] For example, mitaplatin is a dual-targeting prodrug that overcomes cisplatin resistance by selectively attacking nuclear DNA with cisplatin and targeting mitochondria with dichloroacetate (DCA) in cancer cells, resulting a reduced resistance factor (RF) of 3.0 compared to 10.7 for cisplatin.[31]

The activation of Pt(IV) prodrugs involves the reduction of the Pt(IV) center to Pt(II) by bio-reductants such as sodium ascorbate, glutathione (GSH), L-cysteine, and L-methionine. This reduction process can occur through either an inner-sphere or outer-sphere electron transfer mechanism.[11,35,36] Upon reduction, the axial ligands that are in a *trans* position to the Pt(IV) center are typically detached (Scheme 1). Recent studies have shown that the structures of Pt(IV) complexes and the types of reducing agents employed can influence the structures of resulting Pt(II) products, and multiple Pt(II) species can be formed.[22,35,37,38] To measure these reduction processes, both pseudo-first-order and second-order kinetic laws have been employed. Pseudo-first-order kinetics are commonly utilized for reduction measurements, where the reaction occurs with a significant excess of the reducing agent compared to the Pt(IV) complex.[39–42] This approach is often used to simulate the intracellular environment, where reducing agents are typically much more abundant than Pt(IV) complexes. The application of the second-order kinetic law is typically employed when the signal from the Pt(IV) complex is affected by a high concentration of the reducing agent or when investigating the

Ka-Yan Ng

Ka-Yan Ng obtained her B.Sc. in Chemistry (2021) from City University of Hong Kong. Currently, she is a Ph.D. candidate at the City University of Hong Kong under the supervision of Prof. Guangyu Zhu. Her research efforts are on the synthesis and development of photoactivable Pt(IV) and Pt(II) anticancer agents.

Weikang Xu

Weikang Xu received her B.Sc. in Pharmaceutical Preparation from China Pharmaceutical University in 2022. Currently, Weikang Xu is pursuing an M.Sc. in Chemistry at the City University of Hong Kong, where she was supervised by Professor Guangyu Zhu. Her research topic is the determination of possible synergistic effects between platinum anticancer drugs and carbon monoxide-releasing agents.

impact of varying concentrations of the reducing agent on the reduction rate.[43,44]

The reduction step is considered crucial for the activation of these complexes.[45–47] The efficacy of Pt(IV) prodrugs as anticancer agents heavily relies on their reduction profile. If premature activation occurs, the advantages of Pt(IV) prodrugs in addressing the limitations of Pt(II) drugs may not be fully utilized. Conversely, if the reduction rate is significantly slow, the Pt(IV) prodrugs cannot be efficiently activated, and their latent cytotoxic activity remains unreleased. For example, ormaplatin (Fig. 2) has severe neurotoxicity as a result of rapid reduction to the active Pt(II) form, thereby rendering it unable to mitigate the typical side effects associated with Pt(II) drugs.[48] In contrast, iproplatin (Fig. 2), which features two hydroxido axial ligands and a rather negative reduction potential, exhibits resistance to reducing agents, potentially explaining its lack of superior efficacy compared to cisplatin or carboplatin.[36,49–51] Satraplatin and LA-12 (Fig. 2), however, have shown promising outcomes in preclinical studies. These compounds possess favorable properties that ensure stability in the bloodstream and efficient activation upon penetration into cancer cells.[11,52–56]

Therefore, a considerable amount of research has been dedicated to investigating the reduction properties of Pt(IV) prodrugs.[22,32,35,57] A comprehensive understanding of the reduction scenarios of Pt(IV) complexes and the principles behind the reduction is essential for the rational design of innovative Pt(IV) prodrug candidates. To effectively track and analyze the reduction process, different analytical techniques, including ultraviolet–visible (UV-Vis) spectroscopy, high-performance liquid chromatography (HPLC), nuclear magnetic resonance (NMR) spectroscopy, X-ray absorption near edge spectroscopy (XANES), and fluorescence spectroscopy, have been employed. These methods are favored for studying the fate of Pt(IV) complexes in buffer systems or at a cellular level, which provide valuable insights into predicting the cytotoxicity of Pt(IV) complexes, exploring the mechanisms of their cellular activation, and facilitating the development of new Pt(IV) prodrugs for cancer treatment.

In this review, we summarize recent advances in techniques used to monitor the reduction profiles of Pt(IV) complexes. Firstly, we delve into the fundamental principles underlying the techniques employed to track the reduction process of Pt(IV) prodrugs to their Pt(II) counterparts. Furthermore, we summarize and discuss the various techniques utilized to investigate the reduction progress of Pt(IV) complexes in aqueous solutions and at the cellular level. Specifically, we highlight the scope of applications, advantages, and disadvantages of each method. Finally, we offer a concise summary along with a critical evaluation. This review aims to equip researchers with a comprehensive understanding of strategies for monitoring the activation of Pt(IV) prodrugs and shed light on the underlying mechanisms of prodrug activation.

2. Overview of detection principles

According to crystal field theory, the d orbitals of the Pt atom, whose electronic configuration is $[Xe]4f^{14}5d^{9}6s^{1}$, initially feature degeneracy without splitting. Upon oxidation to Pt(II), they adopt a d^8 configuration and undergo d orbital splitting when ligands approach.[58,59] The d^8 Pt(II) drugs prefer a square planar geometry as all eight d-electrons are paired in the lower-energy orbitals, rather than populating the higher-energy t_{2g} set of tetrahedral orbitals (Fig. 3A and B). Additionally, square planar Pt(II) drugs, known for their high crystal field splitting energy surpassing the pairing energy, typically exhibit low-spin configurations. The Pt(IV) prodrug also adopts a low spin configuration due to the larger crystal field splitting energy Δ_o, leading to the pairing of the fourth to sixth electrons in the t_{2g} orbitals; while the hybridization of the two vacant 5d orbitals with the vacant 6s and three of the 6p orbitals results in the formation of six d^2sp^3 hybrid orbitals, promoting the adoption of octahedral geometries in Pt(IV) prodrugs (Fig. 3C). During the reduction of Pt(IV) prodrugs to Pt(II) species, the geometry of the platinum center transforms from octahedral to square planar.[35,60,61] This change in coordination geometry induces a reorganization of electrons around the platinum center, which can be applied as the basis to monitor the reduction of Pt(IV) complex.

For instance, UV-Vis spectroscopy can be applied to monitor the reduction of Pt(IV) complexes. The reduction of simple Pt(IV) complexes containing axial ligands lacking UV absorbances can be monitored by observing the decrease in their ligand-to-metal charge transfer (LMCT) band. The electron transition of Pt(IV) complex from a ligand orbital to a metal d-orbital results in a more intense and red-shifted LMCT band compared with its Pt(II) counterpart, which can be attributed to several factors.[11,62] The relative electron deficiency and presence of two vacant d orbitals in Pt(IV) prodrugs, compared to Pt(II) drugs, favor a higher likelihood of accepting electrons from the ligand, resulting in a more intense LMCT band in Pt(IV) prodrugs.[62–65] The reduced

Guangyu Zhu

Guangyu Zhu obtained his B.Sc. in Chemistry from Peking University (2002), where he developed a strong passion for biological chemistry and drug discovery. He obtained a Ph.D. in Biological Chemistry from the Department of Chemistry at the University of Pittsburgh (2007) and subsequently did his postdoc at the Massachusetts Institute of Technology (MIT). He joined the City University of Hong Kong in 2011 and currently he is a Professor. His research interest lies at the interface of chemistry and biology, focusing on anticancer drug development and mechanism.

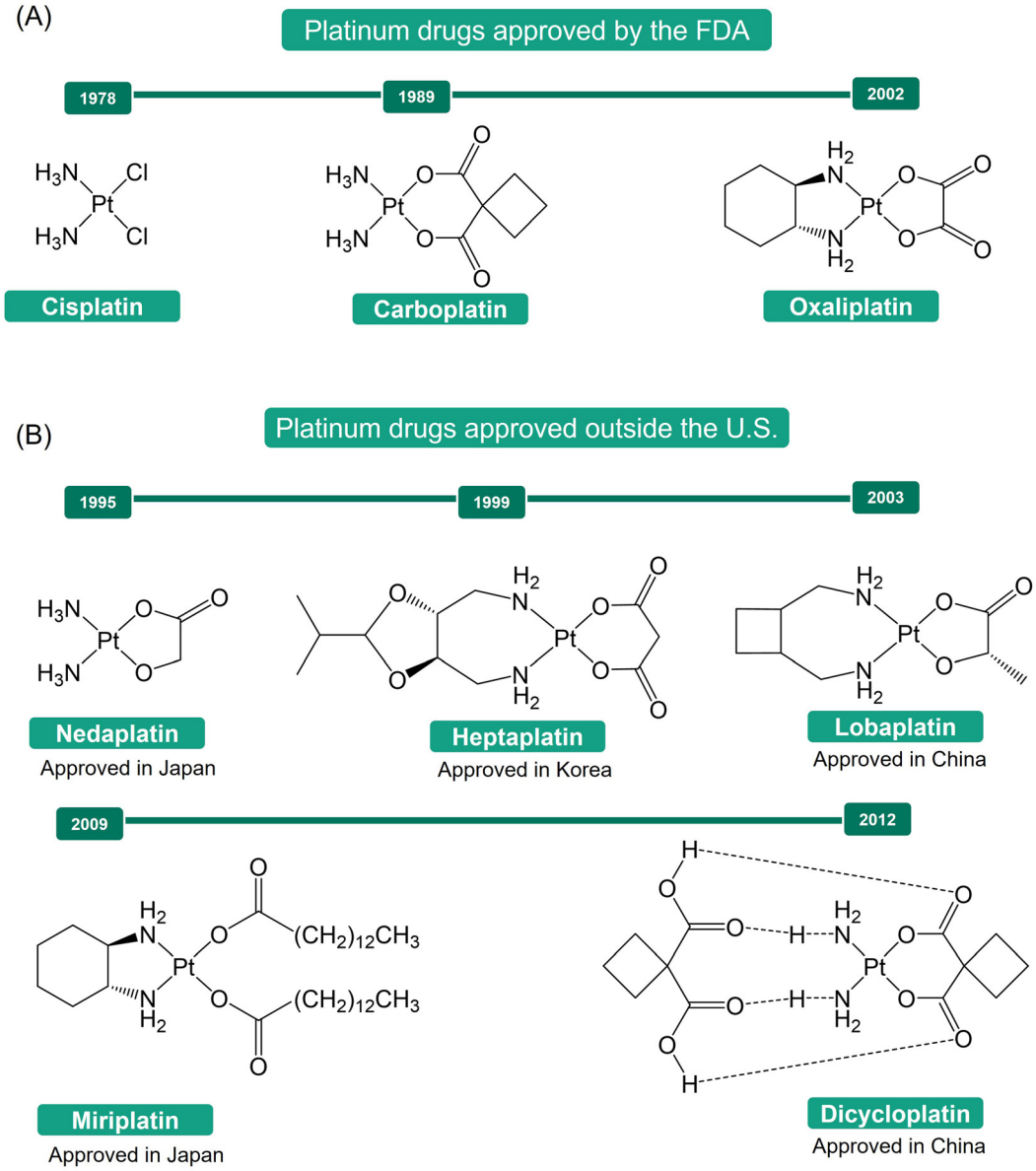

Fig. 1 The chemical structures of clinically approved platinum anticancer drugs.

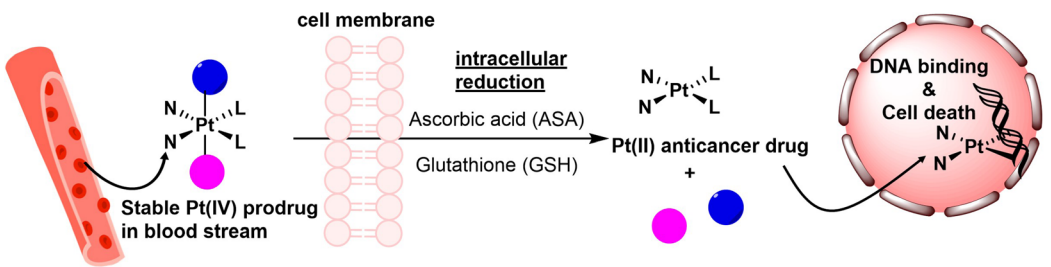

Scheme 1 Proposed activation pathway of Pt(IV) prodrugs in cancer cells.

energy gap between the ligand and metal orbitals in Pt(IV) prodrugs, compared to Pt(II) species, leads to the absorption of red-shifted UV light during the LMCT process (Fig. 3B and C). Accordingly, characteristic absorption bands of Pt(IV) complexes appear in the UV or visible spectrum. Monitoring the decrease in intensity of the LMCT band in Pt(IV) complexes

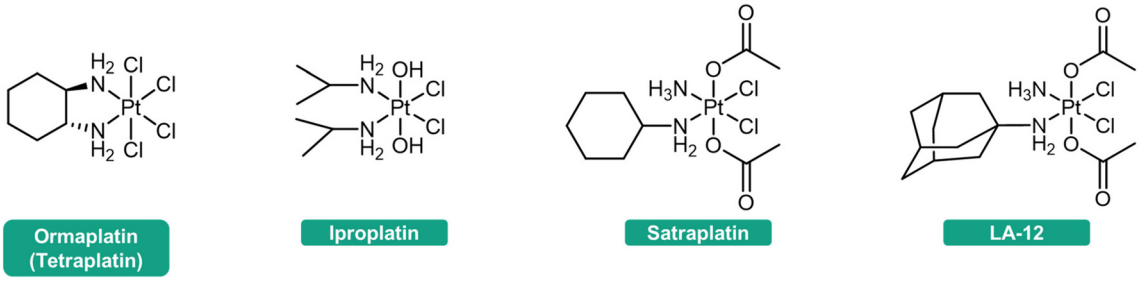

Fig. 2 Structures of Pt(IV) prodrugs in clinical trials.

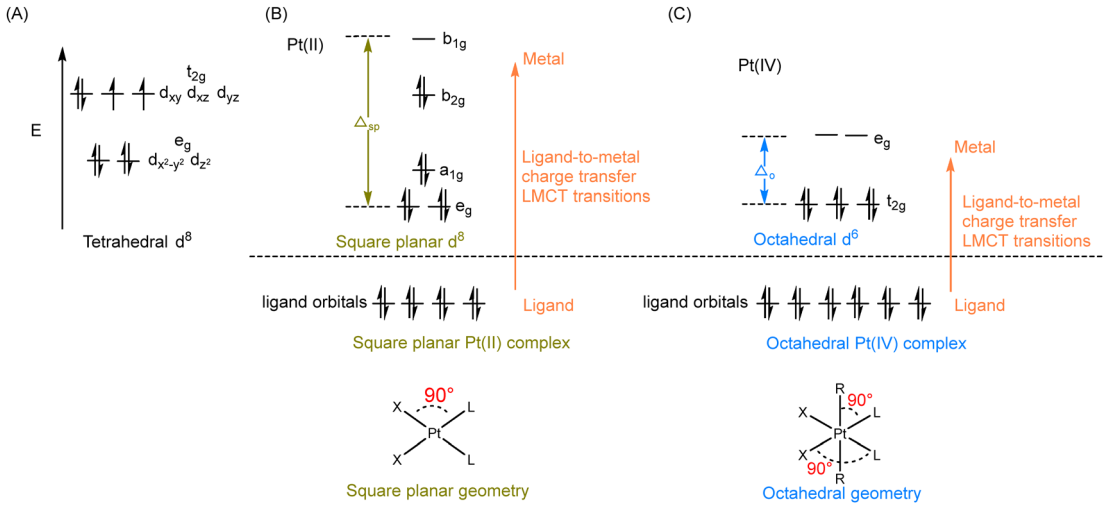

Fig. 3 (A) The d-orbital splitting diagrams for tetrahedral d^8 complexes. (B) The d-orbital splitting diagrams and the ligand-to-metal charge transfer (LMCT) (upper), as well as the geometry (lower) of square planar d^8 Pt(II) drugs. (C) The d-orbital splitting diagrams and the ligand-to-metal charge transfer (LMCT) (upper), as well as the geometry (lower) of octahedral d^6 Pt(IV) prodrugs.

before and after reduction enables rapid determination of the extent of reduction (Fig. 4A).

In cases where Pt(IV) complexes are modified with axial ligands possessing strong UV absorbance, their intrinsic UV absorbance is often overshadowed. Therefore, high-performance liquid chromatography (HPLC) can be used to monitor their reduction. HPLC separates Pt(II) and Pt(IV) complexes based on their differential hydrophobicity, resulting in distinct retention times in HPLC.[66,67] By measuring the change in peak intensity of Pt(IV) complexes, the reduction process can be accurately monitored (Fig. 4B).[68,69] The identification of reduction products, including the Pt(II) counterparts and the released axial ligands, can be achieved by comparing their respective retention times.

X-ray absorption near edge spectroscopy (XANES) enables the capture of X-ray absorption spectra of Pt(II) and Pt(IV) complexes at the Pt L3 edge, which is caused by the excitation of an electron from the occupied 2p orbital to the unfilled 5d orbital.[70,71] The XANES spectra of Pt(IV) complexes show significantly higher edge heights compared to Pt(II) species (Fig. 4C). In Pt(II) drugs, the electronic configuration of Pt is $5d^8$, whereas Pt(IV) exhibits two additional vacancies in the d-shell, resulting in a configuration of $5d^6$ (Fig. 3B and C).[35] Lytle *et al.* attributed the disparities in peak heights to the greater number of unoccupied d states in Pt(IV) complexes. The lower occupancy of the 5d orbitals increases the statistical probability of transitions to these states, thereby intensifying the L3 edge.[70,72] Leveraging these differences in peak height, XANES proves to be a valuable tool for monitoring the reduction of Pt(IV) complexes and discerning the varying oxidation states of platinum.

The reduction of Pt(IV) complexes induces changes in the chemical environment surrounding the Pt nucleus, which consequently causes a variation in the chemical shift of the Pt atom in nuclear magnetic resonance (NMR) spectra.[73–76] In addition, when Pt is conjugated to ligands, it influences their chemical environment, leading to differential chemical shifts compared to the free ligands.[77,78] Moreover, this conjugation often results in the splitting of NMR peaks in ligands due to coupling interactions with platinum or other coordinated ligands, resulting in characteristic split patterns that distinguish them from free ligands.[39,79] The chemical environment of non-leaving groups in Pt(IV) prodrugs also differs from that in Pt(II) drugs.[77,80] NMR spectroscopy utilizes these vari-

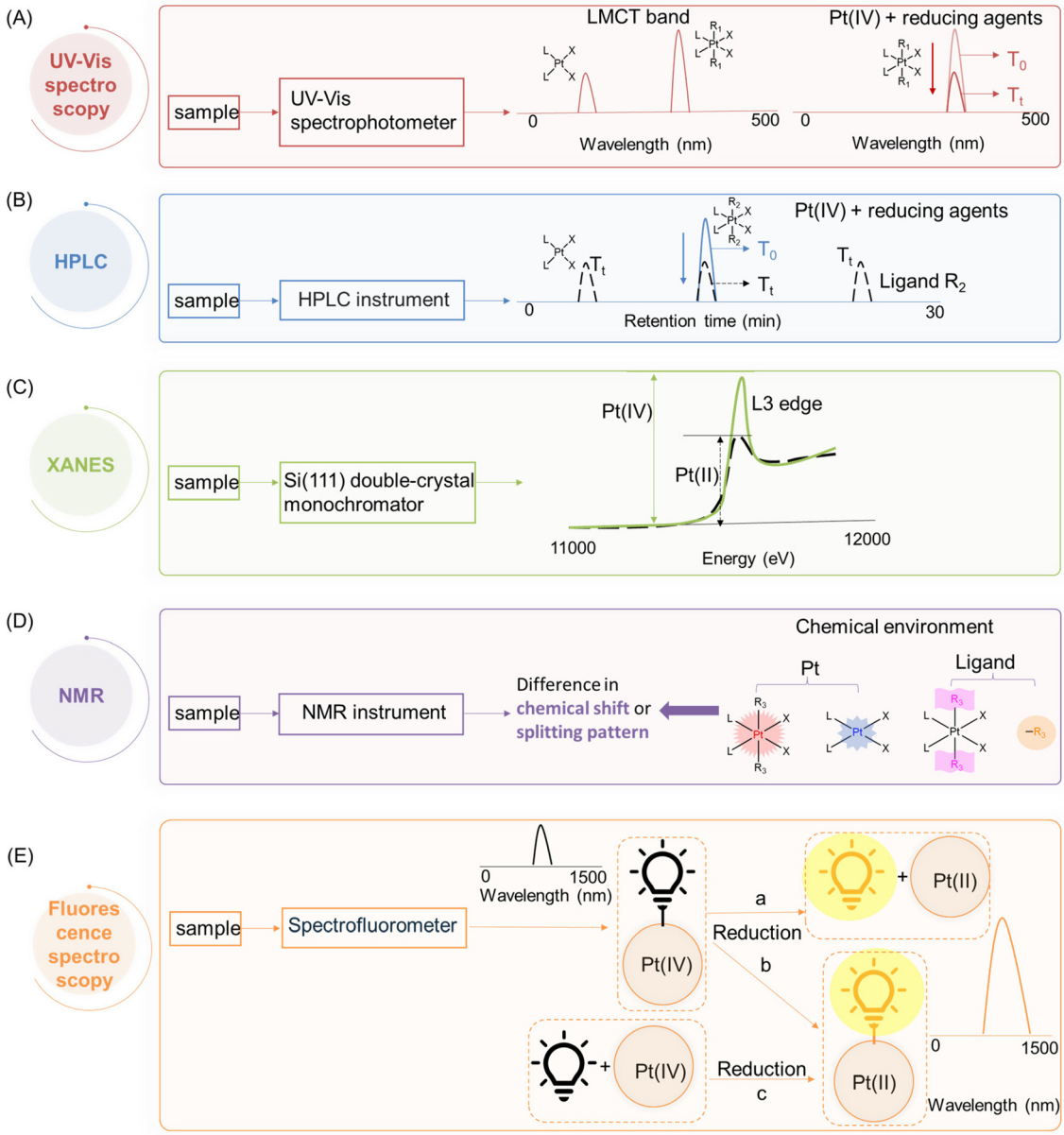

Fig. 4 The layout for detection principles and techniques.

ations to determine the reduction of Pt(IV) complexes and identify the reduction products (Fig. 4D).

In addition to the aforementioned techniques, fluorescence spectroscopy can also be employed to monitor the reduction of Pt(IV) complexes. The attachment of fluorophores to Pt(IV) complexes, whether in an axial or non-leaving position, usually results in a noticeable difference in fluorescence intensity compared to their unbound state. The decrease in fluorescence intensity can be attributed to the phenomena such as homo fluorescence resonance energy transfer (homo-FRET) and the heavy metal effect that occurs upon the conjugation with the platinum centers.[81,82] Conversely, the reduction of Pt(IV) complexes is accompanied by an enhancement in fluorescence intensity, which can be attributed to either the generation of free fluorophores (Fig. 4E-a) or a reduced quenching effect exerted by the Pt(II) center on the fluorophore (Fig. 4E-b), thereby offering a direct visualization of the reduction process both extracellularly and intracellularly.[83,84] Furthermore, an exogenous fluorescent probe can be specifically designed to interact exclusively with Pt(II) species, whereby the turn-on of its fluorescence is observed upon reaction with the Pt(II) center (Fig. 4E-c).[85,86] Such fluorescent probes generally incorporate soft bases, such as sulfur, which prefer bonding to the Pt(II) center that is classified as soft acid, aligning with the principles of the Hard–Soft Acid–Base (HSAB) theory.[1,87]

3. Techniques used to monitor the reduction of Pt(IV) complexes

3.1 Ultraviolet–visible (UV-Vis) spectroscopy

The reduction kinetics of Pt(IV) complexes have often been investigated using UV spectroscopy.[41,68,88–95] As mentioned above, the basis for using UV spectroscopy is that Pt(IV) prodrugs exhibit a more intense and red-shifted LMCT band compared with their Pt(II) counterparts.[11,62] The wavelength of the LMCT band is influenced by the overall configuration (*i.e.*, *cis* and *trans* geometry) of the Pt(IV) prodrugs[62,64,65] and the inherent properties of coordinating ligands (*e.g.*, electron-donating and steric characters).[62,63] During the activation process, the intensity of the LMCT band in Pt(IV) complexes decreases due to the detachment of axial ligands. For example, the band of complex **1** centered at 304 nm exhibits a predominantly LMCT (py → Pt, N_3) character (Fig. 5A and B). Following UVA exposure, this complex undergoes reduction.[96]

To monitor the reduction of Pt(IV) complexes, the initial step involves determining the working wavelength for each tested Pt(IV) by recording their spectra across a wide range of wavelengths. Subsequently, the reduction reaction is initiated by mixing the Pt(IV) complexes and reducing agents in quartz cuvettes. For most kinetic measurements, pseudo-first-order conditions are employed, with a minimum of 10-fold excess of the reducing agent used. The reduction of Pt(IV) complexes is then studied spectrophotometrically by tracking the decrease in the LMCT band at a specific wavelength over time at a specific temperature. To obtain the rate constant, plots of $\ln(A_t - A_\infty)$ *versus* time are generated, where A_t represents the absorbances at time t, and A_∞ represents the absorbance at infinity. These plots are constructed at wavelengths where the absorbance decreases maximally. By analyzing these plots, the reduction rate of Pt(IV) complexes can be determined.[92]

Choi *et al.* conducted a study utilizing UV spectroscopy to monitor the reduction of complex **2** (Fig. 5B) in the presence of a 10-fold excess of ascorbic acid.[41] The reduction process was assessed by measuring the decrease in absorbance (A_t) of the Pt(IV) complex at 330 nm (Fig. 5C). The reduction of complex **2** by excess ascorbic acid followed a pseudo-first-order pattern, as evidenced by the linear plot of $\ln(A_t - A_\infty)$ *versus* time, which exhibited a high coefficient of determination (R^2 = 0.998; Fig. 5D). The slope of this plot provided the pseudo-first-order rate constants. The authors employed this method to measure the reduction rate constants of seven other complexes (Fig. 6). Their findings revealed that the reduction rate of the Pt(IV) complexes was influenced by two factors: the electron-withdrawing power of axial ligands and the steric hindrance of both axial and equatorial ligands. Specifically, complexes with bulkier and more electron-withdrawing ligands exhibited faster reduction rates.

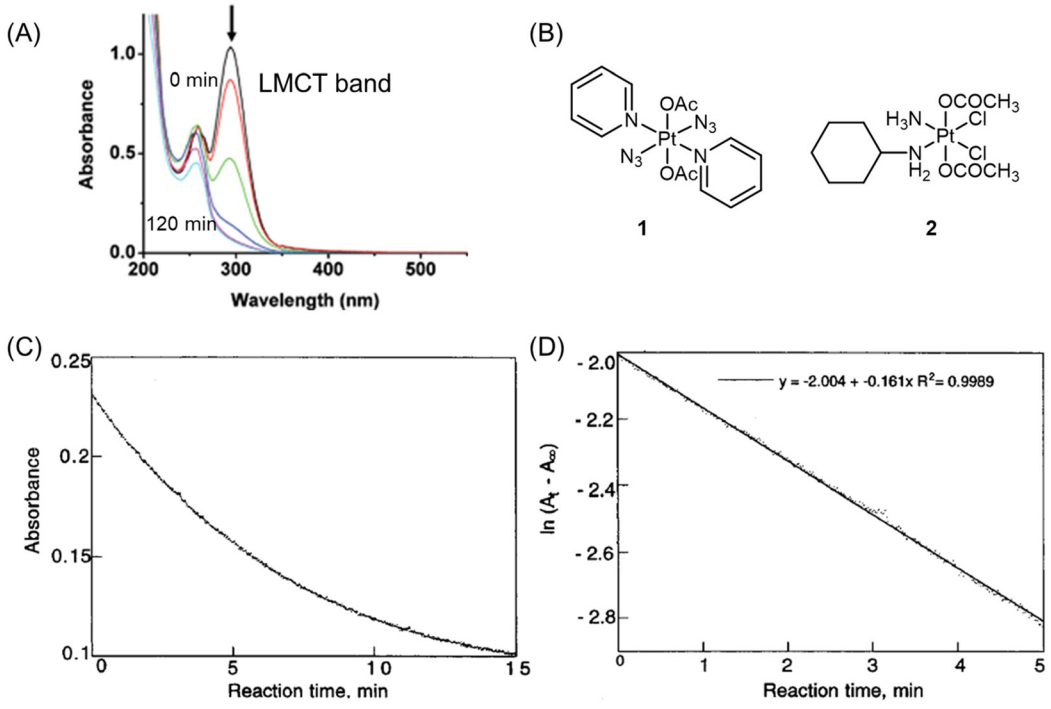

Fig. 5 (A) UV-visible spectra of complex **1** after UVA irradiation for 0, 1, 5, 15, 30, 60, and 120 min. The arrow denotes a decrease in absorbance with increasing irradiation time. Adapted with permission from ref. 96. Copyright 2009, the Royal Society of Chemistry. (B) Chemical structures of complex **1** and **2**. (C) The plot of absorbance at 330 nm *versus* reaction time for complex **2** (0.75 mM) and ascorbic acid (7.5 mM) at pH = 7.1. (D) A plot of $\ln(A_t - A_\infty)$ *versus* time for complex **2** (0.75 mM) and ascorbic acid (7.5 mM) at pH = 7.1. A_t = absorbance at 330 nm at time t. A_∞ = absorbance at 330 nm after 30 min. Adapted with permission from ref. 41. Copyright 1998, American Chemical Society.

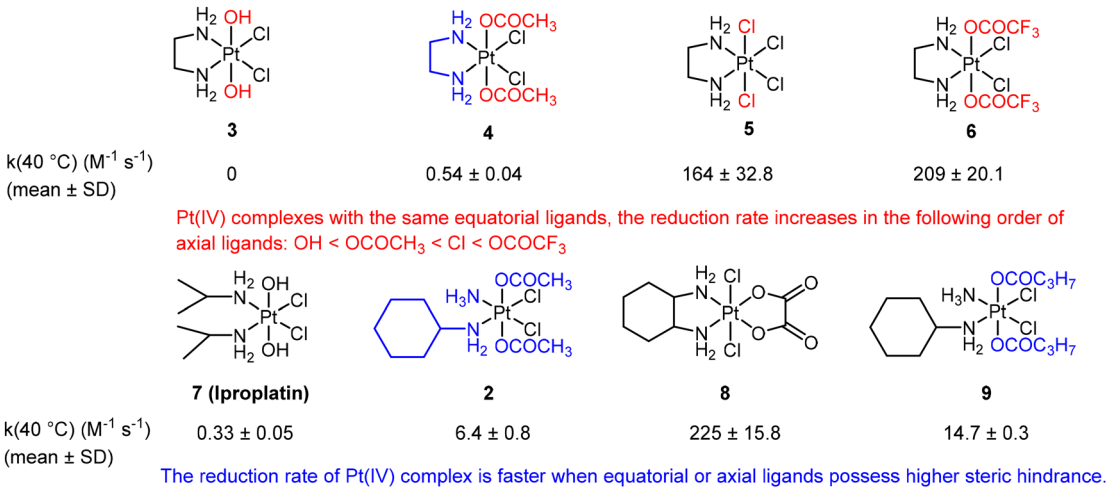

Fig. 6 Chemical structures and reduction rate constants of complexes **2–9**.

UV-Vis spectroscopy offers several advantages in studying the reduction process of Pt(IV) complexes. The non-destructive nature of this technique allows for the reuse of the Pt(IV) sample for further analysis after measurement. Additionally, UV-Vis spectroscopy provides rapid measurements that can capture swift changes in Pt(IV) complexes during reduction, with measurements typically taking only seconds. However, this approach does not provide any information about the identity of the reduction products. Besides, due to the presence of various biomolecules such as proteins, nucleic acids, and pigments in cells that have strong UV-Vis absorption, utilizing this technique to monitor the reduction process of Pt(IV) complexes in live cells is impractical.

3.2 High-performance liquid chromatography (HPLC)

Reversed-phase high-performance liquid chromatography (RP-HPLC) is a widely employed technique for monitoring the reduction of Pt(IV) complexes. This analytical approach provides researchers with the ability to determine whether a Pt(IV) complex will undergo reduction and release the reduction product. Additionally, it allows for the calculation of the rate at which the ligand dissociates from the complex, referred to as its reduction half-life. Therefore, HPLC is an indispensable analytical tool for analyzing Pt(IV) prodrugs before their evaluation in cellular systems.

The concentrations of Pt(IV) complexes used for HPLC analysis usually range from 10 μM to 3 mM.[24,38,97–99] The reduction half-lives ($t_{1/2}$) of Pt(IV) complexes can be determined through several steps. Initially, the HPLC peaks corresponding to Pt(IV) complexes are integrated and analyzed at different time intervals. Subsequently, a linear regression of $\ln(A_t/A_0)$ *versus* time (t) is plotted to calculate the rate constant (k), which is obtained using the pseudo-first-order equation $\ln(A_t/A_0) = -kt$, where A_0 and A_t represent the integrals of the Pt(IV) complex peaks at the beginning and time t, respectively.[100] The reduction half-life can then be calculated using the equation $t_{1/2} = 0.693/k$. The chromatographic peaks of Pt(IV) complexes in the HPLC can be processed using four methods to obtain peak areas that reflect the amount of Pt(IV) complexes reduced at different time points.

3.2.1 Monitoring reduction by absolute peak area in HPLC. The half-life of Pt(IV) complexes can be determined by analyzing the absolute peak area of the complexes at various time points. For example, Gibson and colleagues conducted a study where they conjugated the hydroxyl group of estramustine to Pt(IV) complexes through either a carbonate or succinate bridge, yielding complexes **10** and **11**, respectively.[39] To test the activation scenario of these two complexes, they were exposed to an excess of ascorbic acid at 37 °C in phosphate buffer and their reduction processes were monitored using HPLC. In the HPLC chromatogram, the peak corresponding to complex **10** showed a significant decrease, while the peak of the axial ligand EM gradually increased (Fig. 7A). This indicated that the Pt(IV) complex was being reduced, releasing intact EM and CO_2. In contrast, during the reduction of complex **11**, only the EM-succinate conjugate was slowly released, and no free estramustine was observed (Fig. 7B). The authors measured the absolute area of the peaks of the two Pt(IV) complexes at different time points to determine their respective half-lives. Complex **10** exhibited a half-life ($t_{1/2}$) of 2.2 hours, whereas complex **11** had a half-life of 6.0 hours (Fig. 7C and D). These findings suggest that Pt(IV) complexes with carbonate linkages are more effective in releasing free active moieties compared to those with succinate linkages.

3.2.2 Monitoring reduction by ratio of peak area in HPLC. An alternative approach to using absolute peak area is to utilize area ratios for obtaining reaction kinetics. The total peak area is defined as the area of eluted peaks, excluding those derived from the reducing agents and dead volume.[104] To obtain the normalized integral of the Pt(IV) complex (N_t), the area of the Pt(IV) complex ($A_{t\ \mathrm{Pt(IV)}}$) at different reduction time points is divided by the total peak area ($A_{t\ \mathrm{total}}$) using the equation: $N_t = A_{t\ \mathrm{Pt(IV)}}/A_{t\ \mathrm{total}}$. This area ratio is then used to calculate the reduction half-lives.[100,101,105] For instance, our

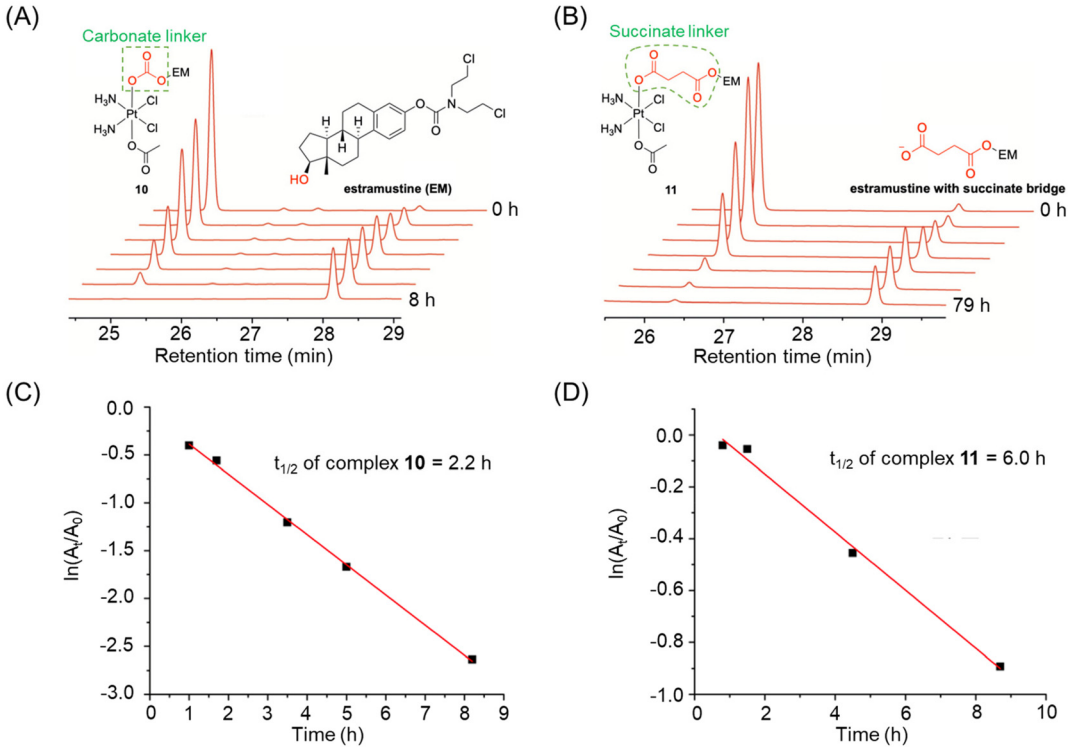

Fig. 7 (A and B) The reduction of complexes **10** and **11**, whose half-lives were calculated based on their absolute peak area at different time points. (C and D) Half-lives of complexes **10** and **11**. Adapted with permission from ref. 39. Copyright 2019, Wiley Online Library.

group employed the area ratio method to determine the half-life of complex **12**.[101] To ensure accurate analysis of the HPLC chromatogram, we eliminated the peak area corresponding to sodium ascorbate and dead volume. Subsequently, we normalized the peak area of complex **12** with the total peak area, which includes peaks from complex **12**, the chalcone ligand, and other minor peaks (Fig. 8A). Within a short span of two hours, the proportion of complex **12** decreased to 71%, and after six hours, this proportion further diminished to 50%. Complex **12** effectively overcomes cisplatin resistance by modulating cellular uptake pathways and reduction rate, exhibiting a decreased RF of 1.8 compared to 4.3 for cisplatin.[101] The area-ratio method is advantageous in eliminating the peak area variation caused by inconsistent sample injection. However, the accuracy of this method is significantly compromised by the issue of peaks overlapping among the reduction products and the Pt(IV) complex.[99] To mitigate this challenge, optimizing the gradient profile or adjusting HPLC settings can enhance the separation efficiency. Furthermore, alternative methods mentioned in the following sections can be taken into consideration.

3.2.3 Monitoring reduction at a wavelength where analytes possess the same molar extinction coefficient in HPLC. Certain Pt(IV) complexes exhibit the same molar extinction coefficient as their reduction products, typically the Pt(II) counterpart or the released axial ligands, at specific wavelengths, known as the isosbestic point. At this particular wavelength, the ratio of the areas of reduction product and Pt(IV) complex equals the ratio of the concentrations of these two species. The remaining amount of Pt(IV) complex can be determined by dividing the peak area of the remaining Pt(IV) complex by the sum of the peak area of the released product and the remaining Pt(IV) complex.[106] For example, we utilized HPLC to assess the photocatalytic ability of rhodamine B (RhB) in the reduction of Pt(IV) complex **13** (Fig. 8B).[102] We selected a wavelength of 303 nm, where complex **13** and oxaliplatin share the same molar extinction coefficient. By utilizing the peak area of oxaliplatin, we were able to determine the percentage of reduced complex **13**. This calculation involved normalizing the peak area of oxaliplatin with the total peak area of both oxaliplatin and the remaining complex **13**.

3.2.4 Monitoring reduction by including an internal standard in HPLC. Including internal standards in the reduction tests is another common practice for obtaining reduction kinetics. By normalizing the peak area of Pt(IV) complexes using internal standards, instrumental variation caused by sample injection can be minimized. An appropriate internal standard for reduction tests should possess the following characteristics: (1) possessing absorbance at the wavelength used for the tested sample, (2) exhibiting stability and inertness in the testing solutions, and (3) showing a retention time that differs from that of the investigated samples. Prior to HPLC analysis, a trace of internal standards is added to the analytes to enable detection and measurement. In this method, the peak area of the Pt(IV) complex at reduction time t is normalized to the peak area of the internal standard, allowing the percentage of

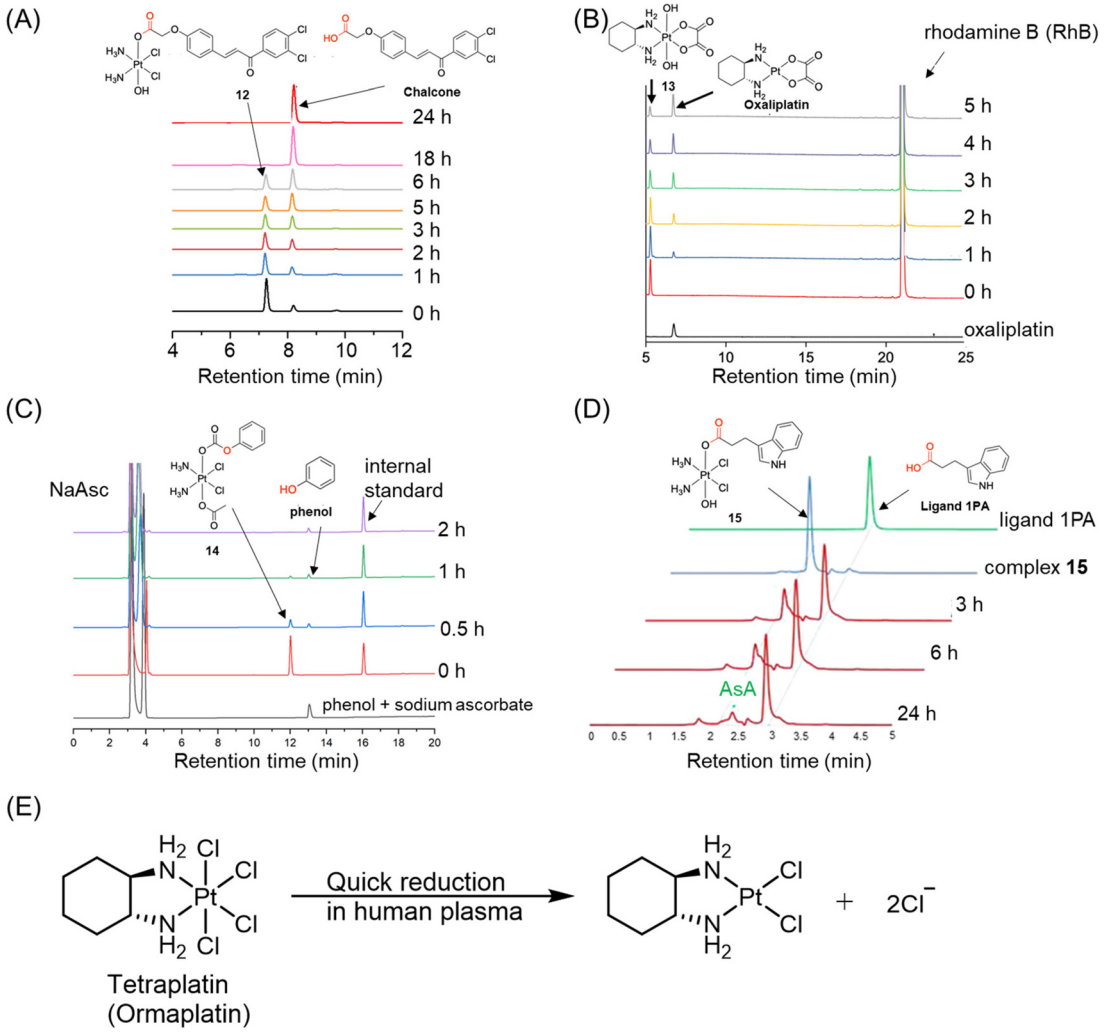

Fig. 8 (A) The reduction of complex **12**, whose half-life was calculated based on its area ratio at different time points. Adapted with permission from ref. 101. Copyright 2019, Wiley Online Library. (B) The reduction of complex **13**, whose peak area was recorded at the wavelength of 303 nm. Adapted with permission from ref. 102. Copyright 2021, the Royal Society of Chemistry. (C) The reduction of complex **14**, whose peak area was normalized with internal standard. (D) The peak overlapping of Pt(IV) complex **15** with reducing agent in HPLC chromatogram. Adapted with permission from ref. 103. Copyright 2016, Springer Nature. (E) The reduction pathway of ormapltin in plasma.

the remaining Pt(IV) complex to be determined. Reduction half-lives can be obtained by plotting a linear regression of the percentage of remaining Pt(IV) complex against time t.[24] For example, a trace amount of triphenylphosphine oxide, possessing the aforementioned characteristics, was used as an internal standard to monitor the reduction of Pt(IV) complex **14** by HPLC (Fig. 8C).[40] The half-life ($t_{1/2}$) of complex **14** was calculated to be 0.5 h. Using internal standards to normalize the peak area is the most effective method for eliminating sample injection variation when calculating the reduction half-life of Pt(IV) complexes.

Ormaplatin (Fig. 2) was among the first Pt(IV) complexes to undergo clinical trials. The reduction of ormaplatin was tracked using HPLC with the aid of an internal standard.[107–109] The reduction half-lives of ormaplatin was determined to be 5–15 minutes in tissue culture medium and a mere 3 seconds in undiluted rat plasma (Fig. 8E).[107,109] This rapid reduction of ormaplatin to its active Pt(II) form, attributed to the presence of axial chloride ligands, resulted in severe neurotoxicity.[48] Consequently, ormaplatin did not progress beyond Phase I clinical trials.

It is worth noting that the reduction of Pt(IV) complexes can be investigated using various techniques. For example, the reduction of iproplatin (Fig. 2) has been extensively studied utilizing HPLC and UV spectroscopy.[50,110,111] Iproplatin possesses hydroxo ligands in the axial positions, which impart resistance to reducing agents.[36] As a result, significant amounts of iproplatin remain unaltered both *in vitro* and *in vivo*, contributing to its low toxicity. Despite undergoing extensive clinical trials ranging from Phase I to III, iproplatin was eventually discontinued due to its inability to demonstrate superior efficacy compared to cisplatin or carboplatin.[50,51]

Although HPLC-UV is an advanced tool for quantitatively detecting the reduction process of Pt(IV) complexes (Table 1),

Table 1 The summary of different methods to process HPLC chromatograms

Methods	Advantages	Disadvantages
Absolute peak area	A convenient method for calculating the reduction rate of Pt(IV) complexes	The results can be affected by inconsistent injection volume
The ratio of peak area	Enhancing the accuracy of calculating the reduction kinetics of Pt(IV) complexes by eliminating variation in sample injection	Peaks overlapping of Pt(IV) complexes with other analytes in the tested solution may affect the calculation of the reduction rate for Pt(IV) complexes
Selecting a wavelength where analytes share the same molar extinction coefficient	This method allows us to determine the percentage of remaining Pt(IV) complexes and that of reduction products simultaneously	This method is inapplicable when molar extinction coefficients of Pt(IV) complexes and reduction products differ
Including an internal standard	Improving the analytical quantification of the peak area of Pt(IV) complexes by eliminating the variation caused by sample injection	An appropriate internal standard should fulfill the following criteria: (1) Having compatible absorption intensity with Pt(IV) complexes (2) Stable during sample preparation and HPLC analysis (3) Its peak should not overlap with the peaks of analytes present in the tested solution

there are several limitations that hinder its broader applications. One limitation is that HPLC with a UV detector can only monitor the release of the reduction product throughout the reduction test if the released product has absorbance in the UV or visible region. However, some commonly used axial ligands in the investigation of Pt(IV) complexes, such as acetate and dichloroacetate, lack UV absorbance.[112,113] Consequently, HPLC with a UV detector cannot be employed to confirm the release and identity of these reduction products. In such cases, alternative detection methods that do not rely on absorbance, such as electrospray ionization (ESI) mass spectrometry and liquid chromatography-mass spectrometry (LC-MS) techniques, can be employed to ascertain their identities.[62,84,114–116] Besides, Pt(II) species in HPLC-UV analysis frequently display low absorbance, posing challenges to their accurate determination. Combining HPLC with ICP-MS could resolve this issue by enabling sensitive detection of Pt species. Moreover, HPLC-ICP-MS allows quantitative monitoring of Pt(II) growth and Pt(IV) reduction, providing precise insights into the conversion process.[117,118] Another limitation arises from peak overlap in the HPLC chromatogram, which can affect data processing. In certain cases, the peaks of reduction products or reducing agents are too close to those of the Pt(IV) complexes.[104] For instance, Erxleben *et al.* analyzed the reduction of Pt(IV) complex **15** using HPLC.[103] The HPLC chromatogram revealed that a portion of the peak of complex **15** overlapped with that of sodium ascorbate (Fig. 8D), posing challenges in obtaining independent peak areas and affecting the accuracy of determining the reduction kinetics of Pt(IV) complexes. The overlap between complex **15** and ascorbate in the HPLC chromatogram can be addressed by using a column with a higher separation efficiency or by optimizing the gradient program to enhance peak separation.

3.3 X-ray absorption near edge spectroscopy (XANES)

X-ray absorption near-edge structure, also known as near-edge X-ray absorption fine structure, is an absorption spectroscopy technique that provides valuable insights into the X-ray absorption spectra (XAS) of condensed matter. X-ray absorption near edge spectroscopy (XANES) can be used to identify the oxidation state of platinum complexes. The XANES spectra of Pt(II) and Pt(IV) species exhibit different edge heights, with Pt(IV) complexes displaying significantly higher edge heights. The peak height ratio, denoted as a/b, where a represents the maximum value of the edge and b corresponds to the local minimum of the edge, in the XANES spectra of platinum complexes, serves as a characteristic feature of the oxidation state (Fig. 9A).[37,42,70,71] Mixtures containing different ratios of the two oxidation states produce a/b ratios that are intermediate between those of the individual oxidation states; these ratios demonstrate a linear relationship with the proportion of the two components in the mixture (Fig. 9B and C).[70,71] Consequently, the peak height ratios can be used to monitor the reduction of Pt(IV) complexes in biological environments.

Hambley *et al.* conducted a study that demonstrated the applicability of XANES in monitoring the reduction of Pt(IV) prodrugs in cells.[71] In their experiment, A2780 ovarian cancer cells were treated with a high concentration of complex **16**, and the reduction process was analyzed using XANES. The reduction from Pt(IV) to Pt(II) and the accompanying change in the edge height were clearly observed. The Pt XANES spectrum of cells treated with complex **16** showed a significantly lower intensity of the edge height after 24 h compared to the spectrum taken at 2 h (Fig. 10A). Based on these observations, the authors calculated the percentage of complexes **16–18** present in the cells (Fig. 10B). The ease of reduction was found to depend on the nature of the axial ligands, denoted as X, in complexes of *c*,*t*,*c*-$[PtCl_2X_2(NH_3)_2]$. Specifically, the order of ease of reduction was found to be X = Cl > OAc > OH.[119] This order was reflected in the extent of cellular reduction observed for the three Pt(IV) complexes after 2 h, where complex **18** was nearly fully reduced, while complexes **16** and **17** still had a substantial proportion remaining as Pt(IV). These results validate the importance of modifying axial ligands to fine-tune the reduction rate of Pt(IV) complexes, thereby offering valuable insights for the rational design of Pt(IV) complexes.

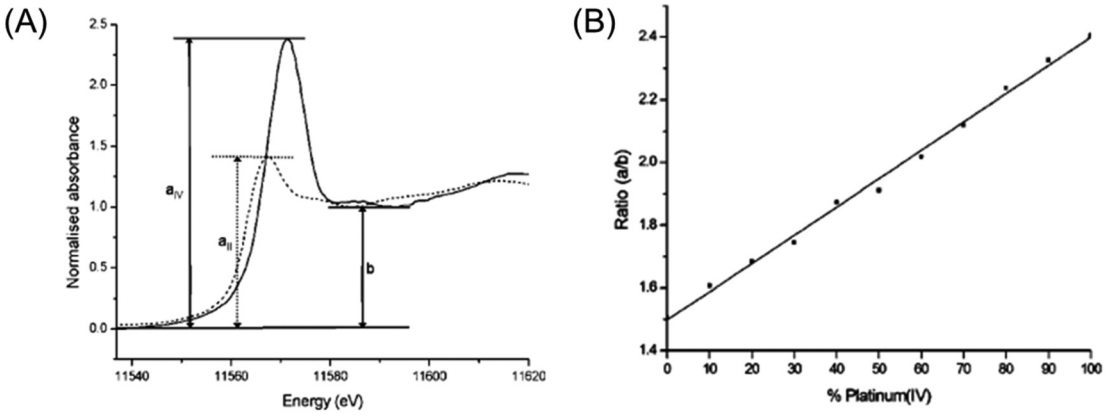

(C)

	Pt(II) complex	Pt(IV) complex		
Structure	Cisplatin	**16**	**17**	**18**
Ratio a/b	1.54	2.41	2.45	2.26

Fig. 9 (A) XANES spectra of Pt(II) (dotted line) and Pt(IV) (solid line) complexes, showing the difference in peak heights for the two oxidation states, and the parameters a and b used in determining the ratio a/b. (B) Linear fit of peak height ratio (a/b) extracted from the Pt(II)/Pt(IV) standard mixtures. Determining the white line height ratio showed a good linear fit (R^2 = 0.99788, P < 0.0001). Adapted with permission from ref. 71. Copyright 2003, American Chemical Society. (C) Experimentally determined peak height ratios (a/b) for XANES spectra of Pt(II) and Pt(IV) complexes.

The analysis of XANES spectra also plays a crucial role in investigating how the Pt(IV) coordination sphere influences the ease of reduction of the platinum center in various biological contexts.[120] In the presence of biological reductants such as ascorbate and cysteine, the Pt(IV) complex **19** with dichlorido equatorial ligands, having a higher reduction potential, exhibited a faster reduction rate ($t_{1/2}$ = 30 min for ascorbate; $t_{1/2}$ = 4.1 h for cysteine) compared with the analogous complex **20** with dicarboxylato equatorial ligands ($t_{1/2}$ = 20 h for ascorbate; $t_{1/2}$ = 27 days for cysteine; Fig. 10C). XANES spectroscopy analysis provided insights into the reduction rates of complexes **19** and **20** within DLD-1 cancer cells. It was observed that both complexes were reduced at similar rates, with 14% and 24% of complexes **19** and **20** remaining, respectively, after 6 h. Despite the unusual kinetic inertness of complex **20** with bidentate oxalato equatorial groups in simple single reductant model systems, its short half-live within cancer cells indicated that the intracellular environment could overcome the stabilizing effects of the tetracarboxylato coordination sphere. The significant variability in kinetic inertness exhibited by complex **20** in different biological contexts has important implications for the design of Pt(IV) prodrugs. While incorporating the tetracarboxylato coordination sphere may render Pt(IV) complexes less susceptible to reduction in the extracellular environment, this study demonstrated that such complexes are rapidly reduced upon entry into cancer cells. Delaying the reduction of the Pt(IV) complexes until they have penetrated the cancer cells may lead to more effective and less detrimental outcomes.

The direct measurement of the relative proportions of two different oxidation states of Pt(II) and Pt(IV) in biological environments using XANES is effective for observing the reduction of Pt(IV) complexes. XANES analysis demonstrates a detection limit of approximately 10 mg kg^{-1},[121] influenced by factors such as the nature of the sample, experimental setup, and the specific element being analyzed. In the case of platinum complexes, clear XANES spectra are typically obtained by exposing cells in one 75 cm^2 flask to the platinum complex at a concentration of 50 μM.[120] However, this technique is time-consuming and requires sophisticated sample preparation, such as collecting and freezing cells, making it unsuitable for

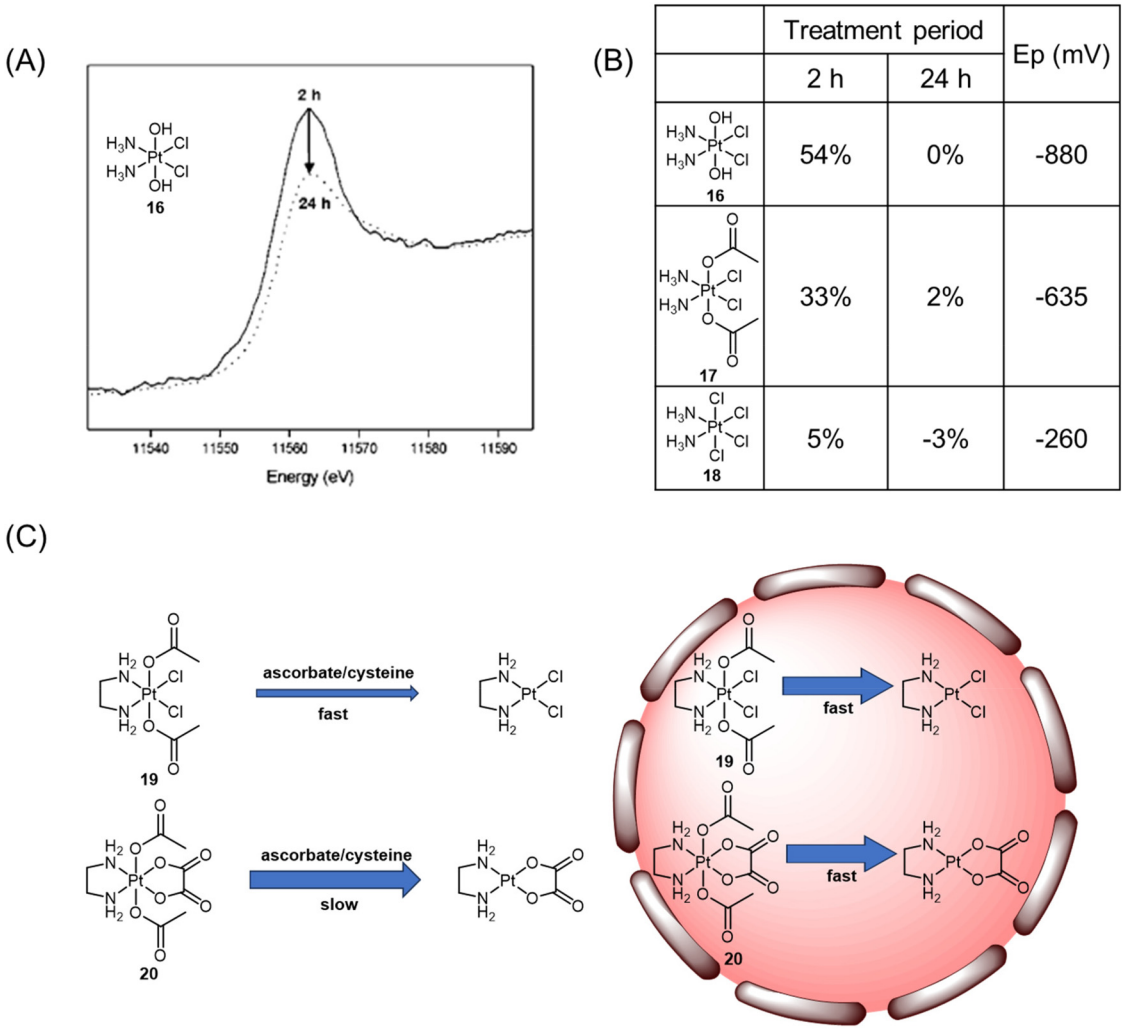

Fig. 10 (A) Normalized XANES spectra of A2780 cells incubated with Pt(IV) complex **16** after 2 h (solid line) and 24 h (dotted line). Adapted with permission from ref. 71. Copyright 2003, American Chemical Society. (B) Proportion of Pt(IV) (±5%) remaining after incubation of complexes with A2780 cells and their reduction potentials (E_p). (C) The reduction of complexes **19** and **20** in various biological contexts.

real-time monitoring of Pt(IV) prodrug reduction in live cells. Additionally, access to the instruments required for XANES analysis is limited, and conducting experiments using synchrotron radiation can be challenging due to the logistical and technical requirements.

3.4 Nuclear magnetic resonance (NMR) spectroscopy

NMR spectroscopy is an informative technique for monitoring the reduction of Pt(IV) prodrugs. It offers several advantages, including the absence of damage to the analysts and the ability to perform time-dependent measurements. NMR can provide insights into the reduction process by analyzing NMR-active isotopes present in Pt(IV) prodrugs, such as ^{1}H, ^{13}C, ^{15}N, ^{19}F, and ^{195}Pt. These isotopes can be scrutinized to track changes during reduction. The choice of NMR technique depends on the structure of Pt(IV) complexes and the interferences from the solution. In numerous studies conducted over the last few decades, deuterated water (D_2O) has been a popular solvent for NMR detection. Unless otherwise specified, the chemical shifts discussed in subsequent sessions were determined using D_2O as the solvent.

3.4.1 ^{195}Pt NMR. ^{195}Pt is the most abundant isotope of Pt, constituting 33.8% of natural abundance. Although its relative sensitivity is only 1% compared to ^{1}H, the range of chemical shift for platinum (δ^{195}Pt) is as wide as 13 000 ppm.[75] This wide range allows for differentiation between different oxidation states of platinum (+2, +4), as the chemical shits can differ by thousands of ppm. Additionally, the substitution of ligands in the Pt complex can lead to chemical shift changes of around 100 ppm from the original values.[74] Hence, ^{195}Pt NMR spectroscopy is extensively used for structural determination and to compare the oxidation state and coordination environment of various Pt complexes. Sadler *et al.* compiled a comprehensive database of δ^{195}Pt values for a broad range of Pt(II) complexes, including clinically approved anticancer drugs like cisplatin and carboplatin. The δ^{195}Pt value for cis-

platin was reported as −2149 ppm, while carboplatin had a value of −1705 ppm. Derivatives of these drugs, where the leaving group ligands (such as Cl and CBDCA) were substituted with other O-, N-, or S-donor ligands, displayed δ^{195}Pt values ranging from −3685 to −1460 ppm.[122] This study provides a valuable reference database of δ^{195}Pt values for Pt(II) anticancer agents, and these values can be utilized when investigating the reduction processes from Pt(IV) prodrugs to Pt(II) drugs.

Dabrowiak *et al.* conducted a study utilizing ^{195}Pt NMR spectroscopy to investigate the reduction of *c*,*c*,*t*-[Pt$(NH_3)_2Cl_2(OH)_2$] (oxoplatin, δ^{195}Pt 853 ppm) in the presence of sodium ascorbate (NaAsc) (Scheme 2A).[123] Cisplatin was confirmed as the major reduction product, as indicated by the ^{195}Pt NMR peak at −2149 ppm, while the presence of other Pt(II) species was also observed, displaying δ^{195}Pt values ranging from −1670 to −1830 ppm.[123] This investigation confirmed that the Pt(IV) complex exhibits "prodrug" properties, as it only binds to DNA after being reduced to cisplatin. Following this discovery, numerous studies have endeavored to track the reduction process of Pt(IV) prodrugs to Pt(II) agents by utilizing ^{195}Pt NMR spectroscopy. Some notable examples include cisplatin-, carboplatin-, and oxaliplatin-based Pt(IV) prodrugs containing axial carboxylate ligands; the corresponding Pt(II) drugs are usually observed in ^{195}Pt NMR spectra (Scheme 2A).[49,100,124,125] In our previous study on pyridinyl-Pt(IV) complex **21**, a unique reduction pathway that involved the detachment of an axial hydroxido and an equatorial chlorine ligand was discovered. This led to the formation of pyriplatin **21-1**, which was identified by ^{195}Pt NMR (Scheme 2B).[38] Besides, Sadler *et al.* reported a photoactivatable azido-Pt(IV) prodrug **22** that yielded Pt(II) active species (**22-1** and **22-2**) upon irradiation, as confirmed by ^{195}Pt NMR spectroscopy (Scheme 2C).[64]

^{195}Pt NMR spectroscopy possesses the ability to distinguish Pt in diverse chemical environments, detect Pt-containing substances *in situ*, and monitor chemical reactions in aqueous solutions. However, a relatively large amount of sample (approximately 10 mM for 600 MHz NMR) is usually required for ^{195}Pt NMR measurement due to its low sensitivity.[22,126]

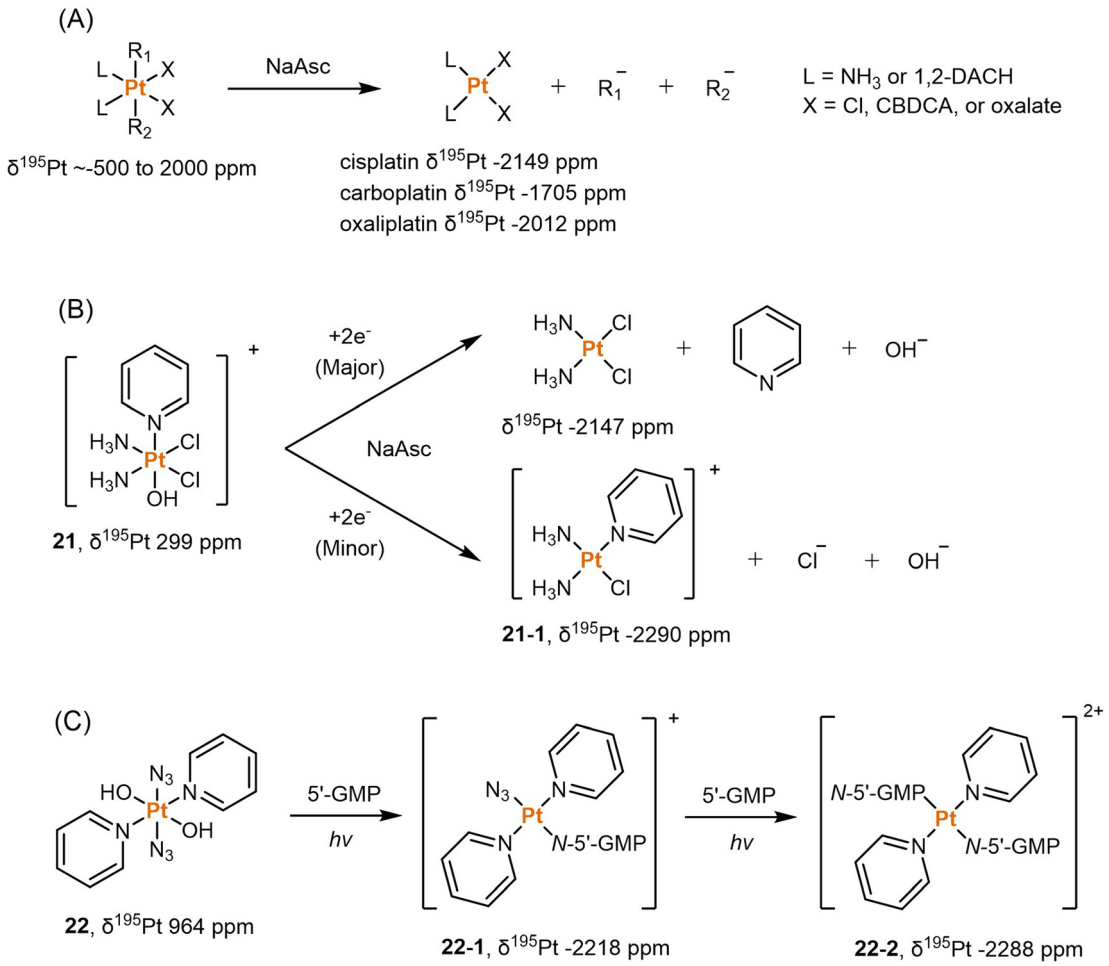

Scheme 2 Monitoring the Pt(II) complexes generated as reduction products by ^{195}Pt NMR. (A) Reduction pathway of typical Pt(IV) complexes (where CBDCA = 1,1-cyclobutanedicarboxylate; 1,2-DACH = 1,2-diaminocyclohexane). (B) Reduction pathway of pyridinyl-Pt(IV) complex **21**. (C) Reduction pathway of azido-Pt(IV) complex **22**.

Moreover, the resolution of ^{195}Pt NMR may not be sufficient to depict all spin-coupling patterns, particularly for Pt complexes coordinated with multiple N- or P-donor ligands.[75] As a result, the Pt peaks in the spectrum can appear broadened, making their assignment challenging.

3.4.2 ^{1}H NMR. In addition to ^{195}Pt NMR spectroscopy, various other NMR techniques are employed to monitor the release of ligands in Pt(IV) complexes during the reduction process. One of the most commonly used techniques is ^{1}H NMR spectroscopy, which probes the hydrogen nuclei. The high natural abundance and sensitivity of the ^{1}H isotope make it an excellent choice for NMR studies. ^{1}H NMR spectroscopy provides valuable information for elucidating the structure of reduction products based on the chemical shifts and integrations of corresponding ^{1}H NMR signals. The short detection time for a single spectrum, typically lasting only a few minutes, allows for time-dependent monitoring of the reduction process using ^{1}H NMR spectroscopy. Moreover, by observing chemical shift changes or increases in peak intensity of specific proton signals in the ^{1}H NMR spectrum, the release of axial ligands or the generation of Pt(II) complexes can be detected.[39,112,127] Additionally, reduction rates can be determined by quantifying the original Pt(IV) complexes and the generated reduction products.

Due to different electron densities, the chemical shifts of protons in coordinated or free ligands can exhibit detectable differences. For example, the loss of axial carboxylate ligands such as benzoate (**23**), acetate (**24**), and succinate (**25**) in Pt(IV) complexes has been observed using ^{1}H NMR spectroscopy (Scheme 3A).[49,128,129] Salassa and co-authors reported that the reduction of complexes **26** and **27** (Scheme 3B) to carboplatin by NADH are photocatalyzed by flavins.[130] ^{1}H NMR signals from the axial acetato (**26**) and succinato (**27**) ligands, as well as the protons in the CBDCA ligand are quantified to determine the conversion percentage.

In some cases, ^{1}H NMR is also helpful in characterizing the structure of resulting Pt(II) products, providing direct confirmation of the reduction process.[131] For oxaliplatin-based Pt(IV) complexes, the hydrogen atoms in their DACH ligands are also usually monitored as indicators of reduction (Scheme 3C).[77,124] For example, Gibson and colleagues investigated the reduction of three oxaliplatin-based Pt(IV) complexes **28–30** by monitoring the ^{1}H NMR signals in the DACH ligand over time (Scheme 3C).[77] Intriguingly, there is no direct correlation between the reduction potentials and the rates of reduction. Complex **30**, with the least negative reduction potential (E_p = −0.48 V), exhibited only a 5% reduction after 12 hours. In contrast, complex **29** (E_p = −0.64 V) had a half-life of approximately 5.5 h, and complex **28**, with the most negative reduction potential (E_p = −0.80 V), underwent the most rapid reduction and possessing a half-life of about 2.5 h. These findings contradict reports for Pt(IV) complexes with N_2Cl_2 coordination spheres, where a correlation between the reduction potential and the rates of reduction exists. Therefore, the electrochemically measured reduction potentials may not necessarily reflect the rates of reduction for Pt(IV) complexes, which hold significance in the design of novel Pt(IV) prodrugs based on oxaliplatin.

Although ^{1}H NMR spectroscopy can offer high-resolution spectra when samples are measured in buffer solutions, it encounters challenges when detecting samples in biological

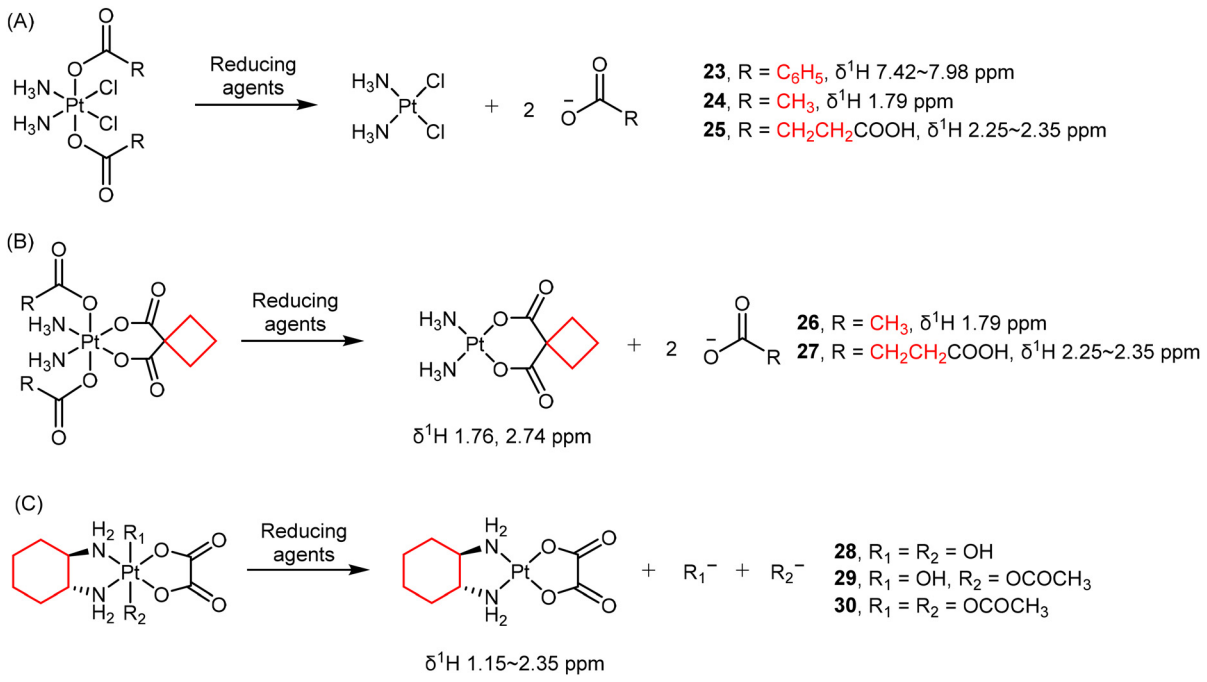

Scheme 3 Monitoring the reduction of cisplatin-, carboplatin- and oxaliplatin-based Pt(IV) complexes by ^{1}H NMR. Respectively, (A) the hydrogen on axial ligands, (B) both axial ligands and CBDCA, and (C) 1,2-DACH were detected.

environments such as cell culture medium or serum due to the high background present. Additionally, the analyte's active H atoms (OH, NH_2, or COOH) may exchange with D in the deuterated solvent, leading to diminished or absent NMR signals.

3.4.3 ^{19}F NMR. The isotope ^{19}F is highly useful in NMR spectroscopy due to its abundance and its ability to exhibit a broad range of chemical shifts (−400 to 400 ppm). Unlike other isotopes commonly found in organisms, such as ^{1}H, ^{15}N, and ^{31}P, ^{19}F does not naturally occur in biological systems except in bones, making it an optimal tool for scrutinizing biological processes within cells using molecules labeled with ^{19}F. In the past decade, there has been a surge in the use of F-containing drugs in clinical applications, and as a result, ^{19}F-NMR spectroscopy has become a vital technique for analyzing pharmacokinetics and pharmacodynamics.

Liu *et al.* designed a Pt(IV) prodrug **31** bearing a 4-fluorobenzoate ligand (FBA) to monitor its reduction process under various biological conditions (Scheme 4A).[78] Upon reduction, the NMR signal of **31** at −107.7 ppm vanished, while a signal corresponding to free FBA at −110.1 ppm emerged. By utilizing ^{19}F NMR spectroscopy, the authors could accurately measure the consumption of the Pt(IV) complex and the release of the free ligand, and were able to determine the reduction rate. More importantly, this approach was also used to track the reduction process of the Pt(IV) prodrug in different types of cells, including A431, A549, and HeLa cancer cells, as well as red blood cells (RBCs) and *Escherichia coli* BL21 (DE3) bacteria cells. The authors detected the release of the FBA ligand from complex **31** over time using ^{19}F NMR spectroscopy. In RBCs, however, a weak ^{19}F signal was only observed after 2 h of incubation, indicating a slower reduction rate. This effect could be attributed to the lower uptake of the Pt(IV) complex in RBCs compared to cancer cells and bacteria.

When F coordinates directly to Pt in Pt(IV) prodrugs, the resulting ^{19}F NMR spectrum typically shows distinct (s + d, J_{Pt-F}) peaks, which arise from the spin–spin coupling between ^{195}Pt and ^{19}F nuclei. Since ^{195}Pt is present at a natural abundance of only 33.8%, approximately one-third of the ^{19}F peak undergoes splitting due to spin–spin coupling, resulting in a doublet peak. The remaining two-thirds of the peak appears as a singlet. In our previous studies, we investigated the reduction of various F-coordinated oxaliplatin-based Pt(IV) complexes using ^{19}F-NMR spectroscopy (Scheme 4B).[24,79] We observed distinct ^{19}F peaks in the spectra ranging from −328.1 to −307.1 ppm, which gradually diminished, while a single peak at −125.3 ppm (representing free F^-) steadily increased. These results indicate that the axial ligands opposite to F significantly affect the reduction rate [carboxylato (**33**) > hydroxido (**32**) > alkoxido (**34**)]. For instance, complex **33** with a benzoato axial ligand is completely reduced to oxaliplatin within 1 hour when treated with 10 equivalents of NaAsc, whereas complex **34** with an axial 2-hydroxyethoxido group remains 95% intact after one-hour incubation with NaAsc, displaying a half-life over 8 h.

The ^{19}F isotope is known for its high sensitivity in NMR spectroscopy and exhibits a wide range of chemical shifts. This sensitivity allows for efficient tracking of the F-containing molecules and assessing the dissociation of F^- or F-containing ligands from Pt(IV) complexes, as it can detect molecular and conformational changes in labeled molecules. In biological settings, ^{19}F NMR provides a non-destructive approach to monitor the reduction of Pt(IV) prodrug in live cells. The wide range of chemical shifts exhibited by ^{19}F, however, poses limitations for its application in 2D NMR spectroscopy, primarily due to hardware requirements. For Pt(IV) complexes, the use of ^{19}F NMR is focused on monitoring the axial F-containing ligands but not the equatorial ligands. As a result, ^{19}F NMR

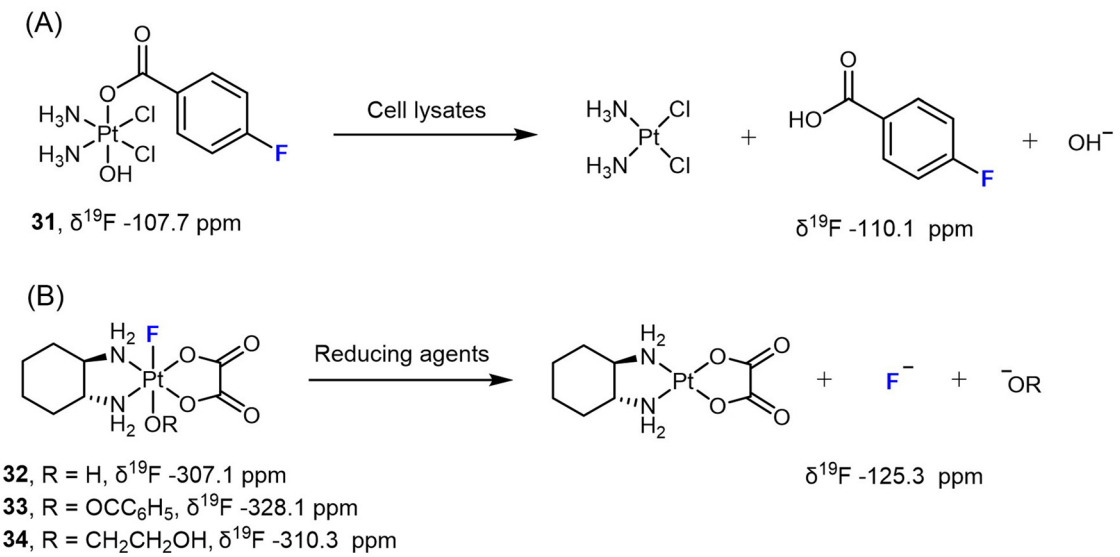

Scheme 4 Monitoring the reduction of F-containing Pt(IV) complexes by ^{19}F NMR. (A) Reduction pathway of 4-fluorobenzoate containing Pt(IV) prodrug **31**. (B) Reduction pathway of F-coordinated Pt(IV) complexes **32–34**.

spectroscopy itself cannot differentiate between hydrolysis and reduction, both of which result in the loss of an F-containing axial ligand.

3.4.4 ^{15}N NMR. Due to the low natural abundance and lower sensitivity compared to ^{1}H, compounds for ^{15}N NMR analysis are usually synthesized using ^{15}N-labelled materials. Over the past few decades, researchers have developed derivatives of Pt(II) drugs that incorporate ^{15}N-amines. This approach allows for insights into the aquation process and binding to nucleotides using ^{15}N NMR spectroscopy.[132,133] The chemical shift (δ^{15}N) of the ^{15}N-labelled amine in Pt(II) complexes is significantly influenced by the substitution of other ligands, whether they are *trans* or *cis* to the ^{15}N-labelled amine. Furthermore, the ^{15}N-labelled amines in Pt(II) and Pt(IV) complexes have distinct chemical shifts,[122] making this approach valuable for monitoring the hydrolysis and reduction process of Pt(IV) prodrugs.

Wong *et al.* employed ^{15}N NMR to examine the reduction of complex *c*,*c*,*t*-[$PtCl_2(^{15}NH_3)_2(COOCH_3)_2$] (**17 (^{15}N)**) by L-cysteine and L-methionine. The authors observed the formation of different products during the reduction process.[128] Complex **17 (^{15}N)** was reduced to cisplatin (^{15}N-labelled) by these reducing agents. Furthermore, L-methionine reacted with cisplatin, resulting in the formation of bidentate Pt(II) complexes in either *cis*- (**17-1**) or *trans*-conformation (**17-2**) (Scheme 5A). Osella *et al.* also investigated the reduction process of complex **17 (^{15}N)** using ^{15}N NMR to analyze the reduction products resulting from sodium ascorbate.[134] The reduction of the Pt(IV) prodrug **17 (^{15}N)** resulted in the clear observation of both ^{15}N-cisplatin (−67.8 ppm) and the mono-aquated product (**17-3**, −65.8 ppm and −88.8 ppm; Scheme 5B). These examples highlight the sensitivity of ^{15}N NMR spectroscopy in detecting and identifying the reduction products of Pt(IV) prodrugs, which can vary depending on the specific reducing agents used. Sadler *et al.* synthesized the ^{15}N-labelled derivative of the photoactivable Pt(IV) prodrug *t*,*t*,*t*-[$Pt(N_3)_2(OH)_2(^{15}NH_3)_2$] (**35**) and tracked its photoreduction pathways using ^{15}N NMR in an acidic solution or PBS buffer.[135] The appearance of ^{15}N peaks (**35-1**, −42.2, −41.3 ppm) in the Pt(IV) region indicated the hydrolysis of azido ligands upon irradiation, followed by reduction to Pt(II) complex **35-2**, accompanied by the emergence of a new ^{15}N peak (−69.6 ppm) (Scheme 5C).

The synthesis of ^{15}N-labelled Pt(IV) complexes remains the main challenge in conducting ^{15}N NMR detection and proves to be both a time-consuming and costly process, given the high expense of materials containing ^{15}N. Consequently, the application of ^{15}N NMR spectroscopy to analyze the reduction process of Pt(IV) prodrugs is limited.

3.4.5 Heteronuclear single quantum coherence (HSQC) NMR. To measure the spin–spin coupling to ^{1}H, the 2D NMR techniques such as [^{1}H,^{13}C] and [^{1}H,^{15}N] HSQC are much more sensitive than their corresponding 1D NMR spectroscopies. These techniques can detect substances in the micromolar range and provide additional information on C–H or N–H bonding, enabling more precise quantification than ^{13}C and ^{15}N 1D NMR spectroscopy. The use of 2D spectra is particularly

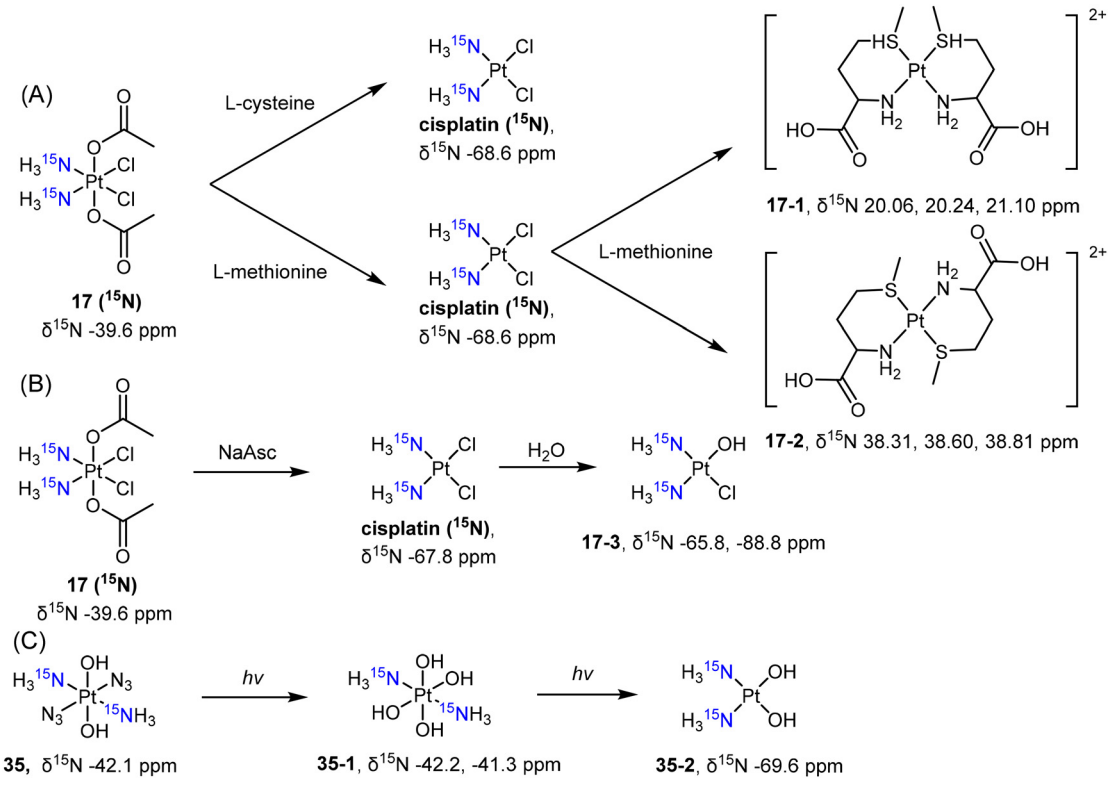

Scheme 5 Reduction pathway of (A, B) ^{15}N-labelled cisplatin-based Pt(IV) complex **17** and (C) diazido-Pt(IV) complex **35**.

critical for analyzing Pt(IV) reduction kinetics. Several examples have demonstrated the utility of 2D NMR in monitoring the reduction process of Pt(IV) prodrugs and its applicability in cell-based assays.

Reducing agents with low molecular mass, such as ascorbate or glutathione, are believed to be responsible for the reduction of Pt(IV) prodrugs in cellular environments. While most studies on the reduction of Pt(IV) complexes utilized ascorbate or GSH as reducing agents, it is crucial to recognize that various other reducing agents present in cells can also activate these complexes. As such, determining which specific cellular reducing agents are involved in the activation of Pt(IV) complexes is warranted. Gibson *et al.* utilized whole-cell extracts as a more realistic model for cellular conditions to study the reduction of Pt(IV) complexes.[136] They synthesized a ^{13}C-labelled Pt(IV) complex *c*,*c*,*t*-[$PtCl_2(NH_3)_2(COO^{13}CH_3)_2$] (**17** (**^{13}C**)) and utilized advanced 2D NMR spectroscopy ([^{1}H,^{13}C] HSQC) to monitor its reduction (Scheme 6A). The authors evaluated the reduction of prodrug **17** (**^{13}C**) in extracts from A2780, A2780cisR, and HT29 cells by monitoring the change in 2D NMR peaks of complex **17** (**^{13}C**) [$\delta(^1H,^{13}C)$ 2.13, 21.22 ppm] and the free acetate ligand [$\delta(^1H,^{13}C)$ 1.94, 22.54 ppm].[136] The reduction curves were plotted, and the rates were calculated based on the quantification of 2D NMR peaks. The study revealed that the aqueous extracts from different cell lines exhibited varying rates of reduction for the same Pt(IV) complex, following the order A2780cisR ($t_{1/2}$ = 36 min) > A2780 ($t_{1/2}$ = 90 min) > HT-29 ($t_{1/2}$ = 130 min). This result suggests that the rate of reduction depends on the reductive capacity, *i.e.*, the contents, of each cancer cell line. Notably, the resistant A2780cisR cells, which have high levels of GSH, showed the most rapid reduction of **17** (**^{13}C**). This observation supports the hypothesis that GSH is responsible for activating Pt(IV) prodrugs in cells. To test this hypothesis further, the authors divided the cell extracts into high and low molecular weight (MW) fractions and examined their ability to reduce the Pt(IV) complex. While the high MW fraction displayed a reduction rate ($t_{1/2}$ = 35 min) similar to that of the whole extracts ($t_{1/2}$ =

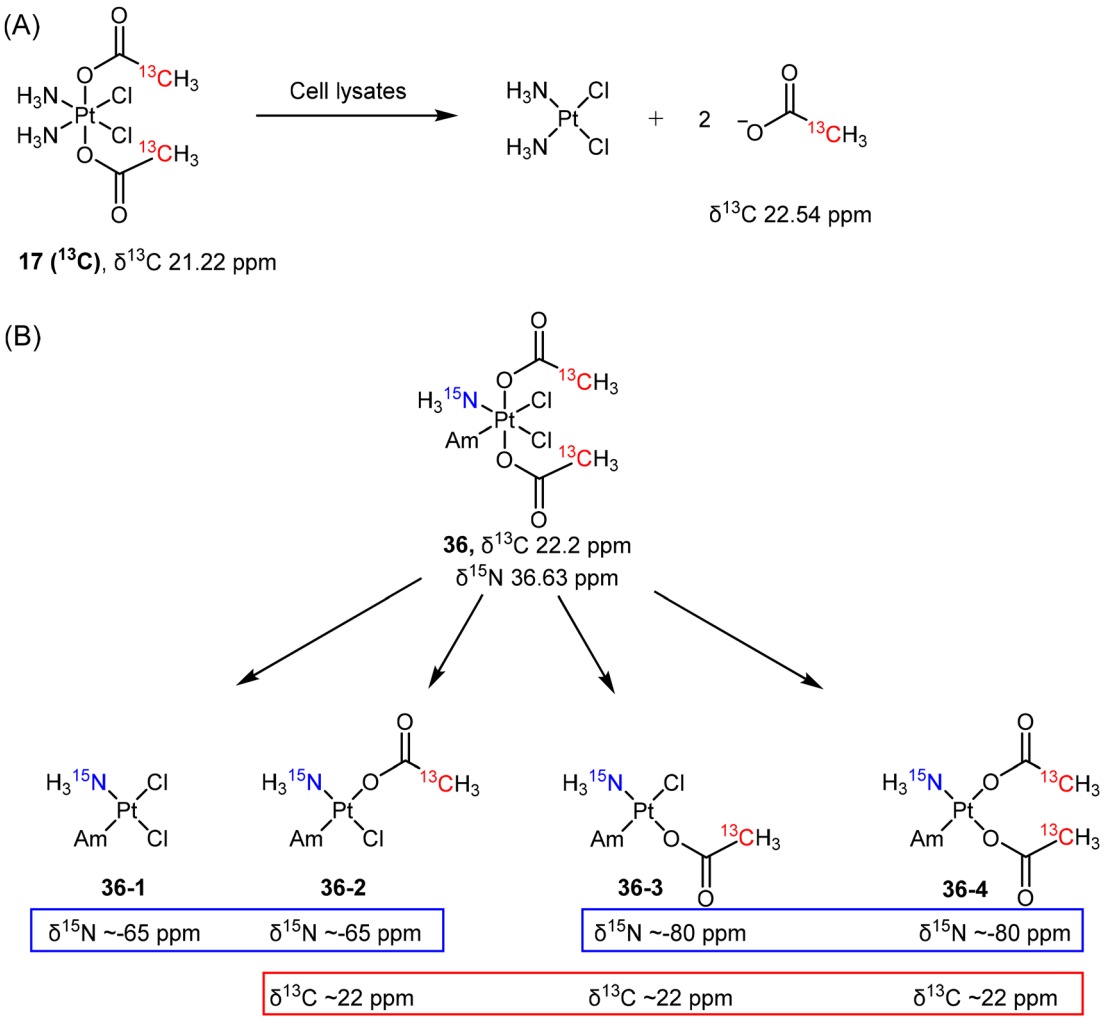

Scheme 6 (A) Reduction pathway of complex *c*,*c*,*t*-[$PtCl_2(NH_3)_2(COO^{13}CH_3)_2$] (**17**, ^{13}C-labelled) detected by [^{1}H,^{13}C] HSQC. (B) Reduction pathway of complex *c*,*c*,*t*-[$PtCl_2(^{15}NH_3)(Am)(COO^{13}CH_3)_2$] (**36**, where Am = cyclohexylamine), detected by [^{1}H,^{13}C] and [^{1}H,^{15}N] HSQC.

36 min), the low MW fraction, which contains both ascorbate and GSH, appeared to have limited efficiency in reducing the Pt complexes (with only 20% reduction after 500 min). The study suggests that the low MW antioxidants, previously considered responsible for reducing Pt(IV) complexes, exhibit lower reduction abilities compared to the whole cell extracts. Hence, it is reasonable to conclude that an aqueous solution containing a single reducing agent (such as GSH, cysteine, or ascorbic acid) may not adequately model the reduction of Pt(IV) complexes within cancer cells.

The reduction mechanisms proposed for Pt(IV) complexes generally suggest that the reduction process yields a single Pt(II) complex by eliminating two *trans*-oriented axial ligands from the octahedral Pt(IV) complex. The reduction of *c*,*c*,*t*-[$PtCl_2(^{15}NH_3)(Am)(COO^{13}CH_3)_2$] (**36**) with axial acetato ligands does not solely proceed by the loss of two axial ligands.[37] When complex **36**, labeled with both ^{13}C- and ^{15}N, was reduced by ascorbate, four distinct reduction products (**36-1** to **36-4**) were obtained and identified using [^1H,^{13}C] and [^1H,^{15}N] HSQC techniques (Scheme 6B).[37] In the [^1H,^{15}N] spectrum, two peaks at $\delta^{15}N$ −65 ppm and two peaks at $\delta^{15}N$ −80 ppm were observed, which indicate that these $^{15}NH_3$ groups were *trans* to either a chlorido or an acetato ligand. In addition, a group of peaks was observed at around $\delta^{13}C$ 22 ppm (Scheme 6B) and differentiated from the peak of free acetate ($\delta^{13}C$ 23.2). Collectively, the four possible reduction products were identified as *c*-[$PtCl_2(^{15}NH_3)(Am)$] (**36-1**), *c*-[$PtCl(^{13}CH_3COO)(Am)(^{15}NH_3)$] (**36-2** and **36-3**, two isomers), and *c*-[$Pt(^{13}CH_3COO)_2(^{15}NH_3)(Am)$] (**36-4**). This example indicates the possibility of losing one or two equatorial ligands during the reduction of a Pt(IV) complex and demonstrates that the use of 2D NMR is effective in identifying the mixtures of reduction products.

In the investigation of Pt(IV) prodrugs' reduction, the [^1H,^{15}N] HSQC technique is more sensitive over [^1H,^{13}C] HSQC, and may show >10 ppm difference in chemical shifts. Arnesano *et al.* studied the reduction of complex *c*,*c*,*t*-[$PtCl_2(^{15}NH_3)_2(COOCH_3)_2$] **17 (^{15}N)** by NADH and cytochrome c (cyt c) (Scheme 7A).[137] The reduction profile was obtained by quantifying the peaks in the [^1H,^{15}N] spectrum, and it was concluded that cyt c accelerated the reduction of the Pt(IV) prodrug in the presence of NADH. Another example reported by Osella involved the reduction of *c*,*c*,*t*-[$PtCl_2(^{15}NH_3)_2$(Gln)$(COOCH_3)$] (**37**), a glutamine-conjugated Pt(IV) complex, by cytosol from A549 cells.[138] The reduction process finished within 1 h and resulted in the formation of ^{15}N-labelled cisplatin, which was observed through [^1H,^{15}N] HSQC at $\delta^{15}N$ −66.8 ppm (Scheme 7B). Intriguingly, when the authors studied the reduction of amidato-Pt(IV) complex *c*,*c*,*t*-[$PtCl_2(^{15}NH_3)_2(COOCH_3)(NHCOCH_3)$] (**38**) in the presence of

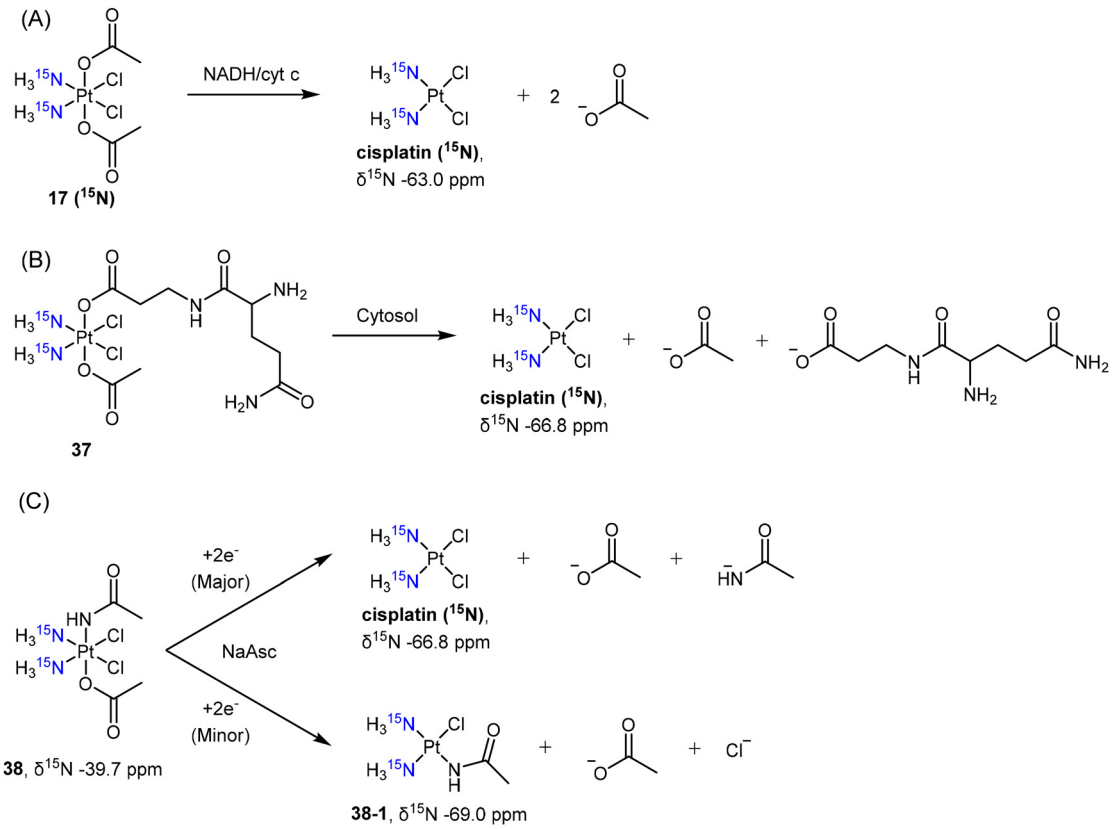

Scheme 7 Reduction pathway of ^{15}N-labelled cisplatin-based Pt(IV) complex **17 (^{15}N)** with (A) axial acetato ligand, (B) complex **37** with glutamine-mimic ligand, and (C) complex **38** with amidato ligand.

sodium ascorbate, a monofunctional Pt(II) complex *c*-[PtCl(NHCOCH$_3$)(^{15}NH$_3$)$_2$] (**38-1**, δ^{15}N −69.0 ppm), as the minor reduction product, was also observed using [^{1}H,^{15}N] HSQC (Scheme 7C).[80]

The diiodo-Pt(IV) complex *t,c*-[Pt(OH)$_2$I$_2$(en)] was initially developed as a photoactivatable Pt(IV) prodrug.[139] Understanding the reduction process and mechanism of this photosensitive complex is essential, and this was achieved through the use of [^{1}H,^{15}N] HSQC with its ^{15}N-analogue **39**. Sadler *et al.* monitored the reduction of complex **39** in the dark in the presence of GSH.[140] Based on the observation of ^{15}N peaks at δ −10.82 and −8.34 ppm after reduction, the authors confirmed that the major reduction product at pH 7 is the ring-opened Pt(II) complex **39-1** (Scheme 8A). When the complex was irradiated in pure water, however, the I ligand was hydrolyzed to OH, leading to the formation of complex **39-2** instead of reduced Pt(II) species, as evidenced by the δ(^{1}H,^{15}N) peak observed at 6.33, −20.07 ppm (Scheme 8B).[141] In contrast, the diacetato complex *t,c*-[Pt(CH$_3$CO$_2$)$_2$I$_2$(^{15}N-en)] (**40**) was found to undergo photoreduction and bind to 5′-GMP, yielding the Pt-GMP adduct *c*-[Pt(5′-GMP)$_2$(^{15}N-en)] (**40-1**), as indicated by δ(^{1}H,^{15}N) peaks observed at 5.72, −30.9 ppm and 5.79, −30.9 ppm (Scheme 8C).

Other photoactivatable Pt(IV) prodrugs reported by Sadler and colleagues include *c,t*-[Pt(^{15}N-en)(N$_3$)$_2$(OH)$_2$] (**41**)[142,143] and *t,t,t*-[Pt(N$_3$)$_2$(OH)$_2$(^{15}NH$_3$)py] (**42**).[144] The azido and pyri-

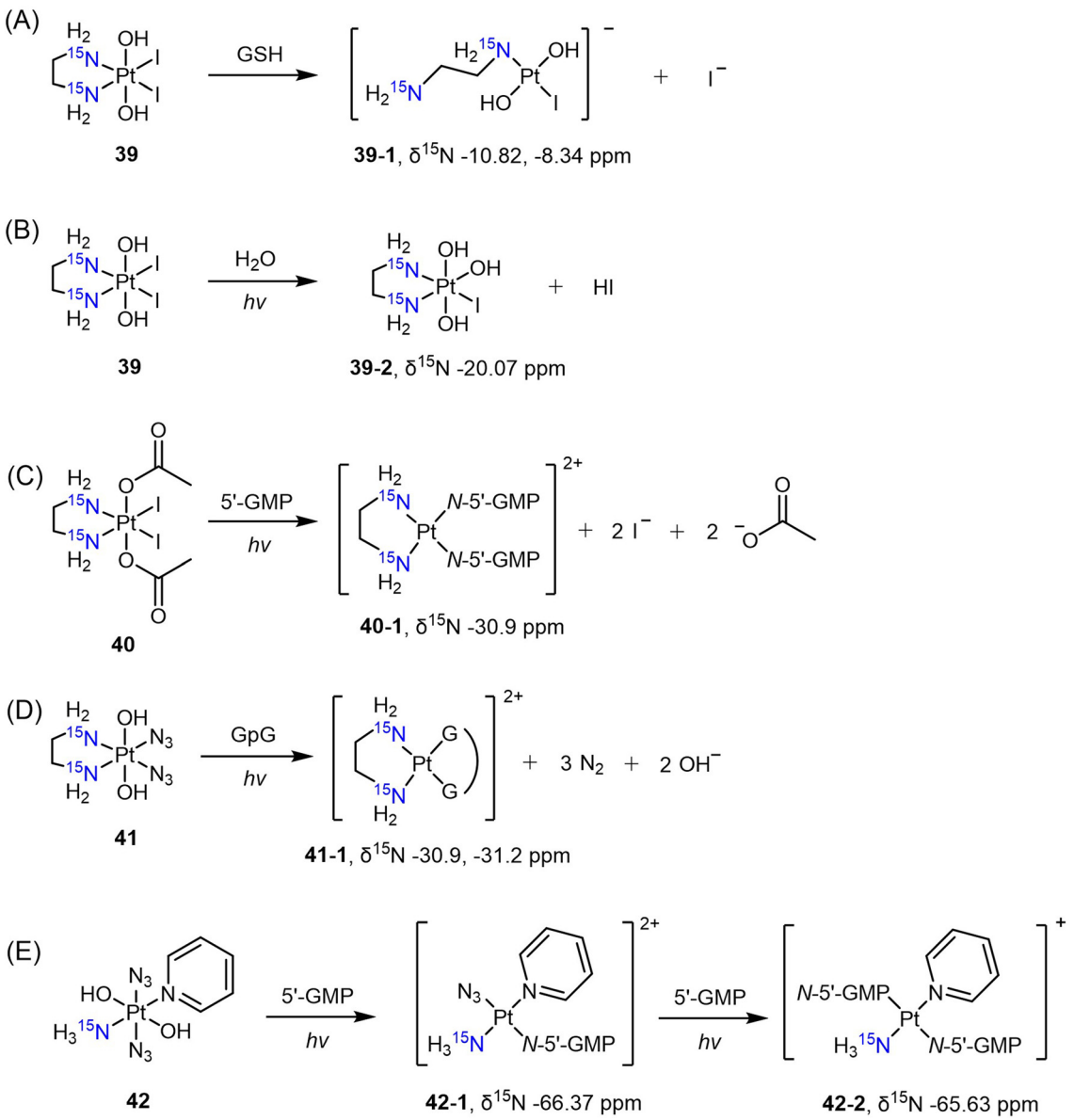

Scheme 8 (A) Reduction of *t,c*-[Pt(OH)$_2$I$_2$(^{15}N-en)] (**39**) by GSH. (B) Photolysis of *t,c*-[Pt(OH)$_2$I$_2$(^{15}N-en)] (**39**). (C) Reduction of *t,c*-[Pt(OH)$_2$I$_2$(^{15}N-en)] (**40**) upon irradiation and formation of 5′-GMP-Pt adduct. (D) Reduction of *t,c*-[Pt(OH)$_2$(N$_3$)$_2$(^{15}N-en)] (**41**) upon irradiation and formation of d(GpG)-Pt adduct. (E) Reduction of *t,t,t*-[Pt(N$_3$)$_2$(OH)$_2$(^{15}NH$_3$)py] (**42**) upon irradiation and formation of mono- and bis-5′-GMP-Pt adduct.

dine ligands, due to the lack of hydrogen atoms attached to these N atoms, cannot be detected by [^{1}H,^{15}N] HSQC. Upon irradiation, complex **41** was reduced to the aquated Pt(II) species within 40 min and bound to a nucleotide d(GpG), resulting in the formation of the chelating Pt(II) adduct *c*-[Pt(^{15}N-en)(GpG)] (**41-1**). The δ(^{1}H,^{15}N) peaks observed at 5.65, −30.9 ppm and 5.56, −31.2 ppm confirmed the presence of this adduct (Scheme 8D).[143] In the presence of 5′-GMP, *t*,*t*,*t*-[Pt(N_3)$_2$(OH)$_2$(^{15}NH_3)py] (**42**) was reduced, yielding the monofunctional Pt(II) adduct *t*,*t*-[Pt(N_3)(5′-GMP)(^{15}NH_3)py] [**42-1**, δ(^{1}H,^{15}N) 4.15, −66.37 ppm] within 5 min (Scheme 8E).[144] Subsequently, a second-step photolysis was initiated, which took one hour, eventually leading to the formation of the bis-5′-GMP adduct *t*-[Pt(5′-GMP)$_2$(^{15}NH_3)py] [**42-2**, δ(^{1}H,^{15}N) 4.42, −65.63 ppm] (Scheme 8E).[144]

The [^{1}H,^{15}N] HSQC technique is highly effective in monitoring the reduction process of Pt(IV) prodrugs by various reducing agents. It also enables differentiation between hydrolysis and reduction during photoreactions. Furthermore, this technique demonstrates remarkable sensitivity and can be employed in biological fluids, with the potential to detect ^{15}N-labeled compounds in live cells.

In analyzing the reduction profiles of Pt(IV) prodrugs, several types of NMR techniques can be used, as summarized in Table 2. The detection limit of NMR spectroscopy is affected by many parameters such as sample volume, sample type, measurement frequency, number of scans, NMR setup, and the specific isotopes being detected.[145] For example, the detection limit of ^{1}H NMR spectroscopy can be as low as 1 ppm when using a 600 MHz instrument and 1024 scans. With the same frequency and number of scans, the detection limit of other isotopes is generally scaled up relative to their sensitivity, as shown in Table 2. The most sensitive NMR techniques include ^{1}H NMR and its 2D variants, such as [^{1}H,^{13}C] and [^{1}H,^{15}N] HSQC. These techniques are commonly utilized for quantification and time-dependent measurements. ^{195}Pt NMR is particularly useful as it directly detects the Pt center, allowing the differentiation of Pt(II) and Pt(IV) complexes in various coordination environments. ^{15}N NMR and [^{1}H,^{15}N] HSQC can help identify the ligands opposite to the ^{15}N-labelled ligand, thereby facilitating the determination of the reduction process of Pt(IV) prodrugs. Furthermore, ^{19}F NMR provides another sensitive method for monitoring the change of ligands in F-containing Pt(IV) complexes in buffered solutions or cells. The choice of NMR spectroscopy depends on specific conditions and research objectives. Overall, this technique is critical in comprehending the reduction of Pt(IV) complexes and is instrumental in the design of novel Pt(IV) anticancer agents.

3.5 Fluorescence spectroscopy

Fluorescence spectroscopy is an advantageous analytical technique due to several key features, including its ability to detect low concentrations of fluorescent molecules with high sensitivity, excellent selectivity that is derived from the unique fluorescence emission spectra of different compounds, and non-invasive and non-destructive nature, which allows for the preservation of sample structure and integrity throughout the analysis process.[81,146–151] These advantages make fluorescence spectroscopy an effective tool for monitoring dynamic processes of Pt(IV) prodrugs, both in test tubes and at the cellular level.[83,85,86,114,152–154] Fluorophores have been conjugated to Pt(IV) complexes to track their reduction process in different biological contexts. It was anticipated that the coordination of fluorophores with Pt(IV) complexes would result in fluo-

Table 2 Summary of different NMR techniques and their applications in monitoring Pt(IV) prodrug reduction

NMR types	Relative sensitivity[a]	Advantages	Disadvantages	Applications
^{195}Pt	0.99	Direct measurement of Pt; can distinguish Pt(II) and Pt(IV)	Less sensitive, not quantitative, requires a large amount of sample	Trace Pt(IV) to Pt(II); identify Pt(II) products from the library of ^{195}Pt chemical shifts[75]
^{1}H	100	Sensitive, quantitative, and informative	Interfered by proton exchange; high background in biological fluid	Quantitatively plot the reduction curve, calculate the reduction rate, and identify free ligand released
^{19}F	83.3	Sensitive, applicable in cell lysates and live cells	Require ^{19}F-containing compound; cannot distinguish hydrolysis and reduction	Monitor the loss of ^{19}F-containing ligands in buffered solutions, cell lysates, or live cells
^{13}C	0.016	High resolution and large range of chemical shift	Require ^{13}C-labelled compound, low sensitivity	No published applications
^{15}N	0.104	Can distinguish Pt(II) and Pt(IV), sensitive to the change of *trans* ligand	Require ^{15}N-labelled compound, low sensitivity	Trace Pt(IV) to Pt(II) and detect ligand exchange
[^{1}H,^{13}C] HSQC	100	Sensitive, quantitative, and present C–H bonding, high resolution, extensive range of chemical shift, and applicable in cell lysates	Require ^{13}C-labelled compound, not applicable to ^{13}C atom without H	Monitor the loss of ^{13}C-labelled ligands and identify reduction products in buffered solutions or cell lysates
[^{1}H,^{15}N] HSQC	100	Sensitive, quantitative, and present N–H bonding. It can distinguish Pt(II) and Pt(IV), and it is sensitive to the change of *trans* ligand and is applicable in cell lysates	Require ^{15}N-labelled compound, not applicable to ^{15}N atom without H	Trace Pt(IV) to Pt(II) in buffered solutions or cell lysates, detect ligand exchange, and identify reduction products

[a] Relative sensitivity is compared to ^{1}H NMR, which is defined as 100.

rescence quenching, which can occur through homo-fluorescence resonance energy transfer (homo-FRET) or the heavy metal effect.[81,82] Reduction of Pt(IV) complex was accompanied by a concomitant enhancement in fluorescence intensity, which, in principle, provides a direct method for visualizing the reduction process, either extracellularly or intracellularly.[83,84,114] Besides, by designing an external probe that exclusively interacts with Pt(II) species, fluorescence can be "turned on" specifically upon reduction of Pt(IV) prodrugs, providing further visualization capabilities.[85,86]

3.5.1 Fluorophores at the axial position. Lippard *et al.* reported Pt(IV) complex **43**, which is a conjugate of fluorescein—an effective fluorescent reporter—with a cisplatin-based Pt(IV) complex. The purpose was to investigate the transformation from Pt(IV) to Pt(II) in cancer cells (Scheme 9A).[114] Once attached to platinum, the probe has diminished fluorescence in the "off" state.[155] A significant 5-fold fluorescence turn-on occurred upon treating complex **43** with the biologically relevant reducing agent GSH. The fluorescence turn-on of complex **43** provided a means to monitor the cellular accumulation and conversion of Pt(IV) prodrugs to Pt(II) species through fluorescence spectroscopy. Treatment of HeLa cells with complex **43** for one hour resulted in a pronounced intracellular green signal, while the axial ligand FL-COOH, which had poor cell permeability, did not produce noticeable intracellular green fluorescence. From these observations, the authors proposed that complex **43** entered cells intact and underwent reduction intracellularly. While the utilization of the fluorescence probe holds the potential for qualitatively monitoring intracellular Pt(IV) reduction, accurately determining the absolute concentrations of Pt(IV) complexes reduced within cells poses a formidable challenge. This challenge arises from the fact that the increase in fluorescence may arise from both the released free fluorescein and the conjugated fluorescein from intact Pt(IV) complexes that continuously enter cells, which is the common limitation for this type of probe.

Recently, our group developed a fluorescent sensor **44** by attaching a BODIPY fluorophore to the axial position of a carboplatin Pt(IV) analogue. This sensor allows for real-time monitoring of the reduction of Pt(IV) complex (Scheme 9B).[83] Upon incubation of the sensor with sodium ascorbate and cell extracts, a fluorescence turn-on effect was observed (Scheme 9C). This turn-on effect resulted from the reduction of **44** and thus, the liberation of the BODIPY ligand, whose fluorescence was previously suppressed when bound to platinum (Scheme 9D). Further investigation revealed that the fluorescence turn-on was predominantly caused by proteins with

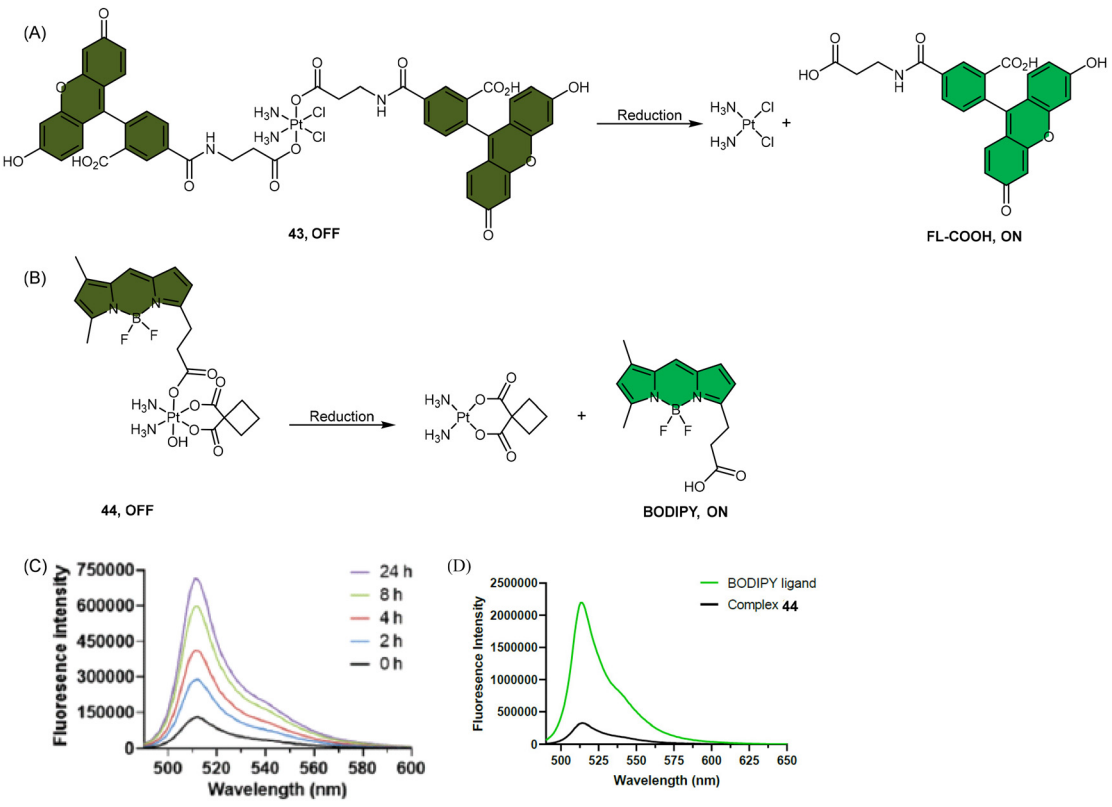

Scheme 9 The Pt(IV) complexes with axial (A) fluorescein ligands (**43**) and (B) BODIPY ligands (**44**) exhibit fluorescence 'turn-on' following the reduction of Pt(IV) complexes and release of the axial fluorophore. (C) The time-dependent emission of 10 μM complex **44** in PBS buffer (pH 7.4) with 1 mM sodium ascorbate and 1% DMF at 37 °C. (D) Emission of 10 μM complex **44** and the BODIPY ligand in PBS buffer (pH 7.4) with 1% DMF. The excitation wavelength is 470 nm. Adapted with permission from ref. 83. Copyright 2022, the Royal Society of Chemistry.

high molecular weights, especially those between 10 and 100 kDa. This finding confirms that high-molecular-weight proteins contributed significantly to the reduction of Pt(IV) complexes. Although the sensor is highly effective in monitoring the reduction of Pt(IV) prodrugs in a real-time mode, it could only be applied to cell lysates due to the rapid secretion of the complex from live cells.

Fluorophores containing carboxylates have been commonly used in Pt(IV) sensors, likely due to the ease of carboxylation during the synthesis of Pt(IV) complexes and the relatively high stability of carboxylate ligands. Expanding the range of fluorophores beyond carboxylates has posed a challenge. Ang and coworkers developed an innovative method to obtain Pt(IV) prodrugs, in which they employed self-immolative 4-aminobenzyl linkers to conjugate a Pt(IV) complex with the OH of fluorophore 7-HMC, thus creating a stable carbamate bridge on the Pt(IV) scaffold **45** (Scheme 10A).[84] Upon reduction of the self-immolative Pt(IV) prodrug **45**, the carbamate ligand detached and underwent decarboxylation and 1,6-elimination processes, resulting in the generation of 4-aminobenzyl alcohol and carbon dioxide. This process also led to the release of 7-HMC and the concomitant restoration of fluorescence emission from the fluorophore. Upon the addition of sodium ascorbate to complex **45**, a time-dependent enhancement in fluorescence emission at 450 nm was observed. Complex **45** underwent complete reduction within 18 hours, displaying a maximum fluorescence intensity at this time point comparable to the equimolar concentration of 7-HMC. Hence, the demonstration of complex **45** establishes the effectiveness of Pt(IV) prodrug and self-immolation strategies in achieving efficient co-delivery of Pt(II) and a bioactive ligand within cells through intracellular reduction. Sedgwick's group utilized a similar method to incorporate the fluorophore resorufin into a Pt(IV) complex, and a fluorescence probe **46** was obtained (Scheme 10B).[156] This carbamate-functionalized probe displayed sodium ascorbate-dependent increases in fluorescence emission intensities. Complex **46** showed potential as a hypoxia-activated prodrug. Under conditions of <0.1% O_2 (hypoxia), the probe displayed the highest fluorescence signal compared to the normoxic condition (21% O_2), indicating that hypoxia was more efficient in inducing the bioreduction of Pt(IV) compounds to Pt(II) species compared to normoxia. Additionally, clonogenic cell survival assays revealed that the complex **46** was significantly more toxic in hypoxic conditions than in normoxic conditions. This hypoxia-activated prodrug contributes to elucidating the factors that affect intracellular reduction of Pt(IV) complexes.

The fluorescence turn-on response resulting from the liberation of fluorophores has been utilized to monitor the reduction of Pt(IV) complexes, and its application can be expanded to indicate the activation of specific pathways in cells, such as apoptosis. Liu and coworkers reported a chemotherapeutic Pt(IV) prodrug **47** in which one axial position was functionalized with an apoptosis sensor composing a tetraphenylsilole (TPS) fluorophore with aggregation-induced emission (AIE) characteristics and a caspase-3-specific Asp-Glu-Val-Asp (DEVD) peptide (Scheme 11).[157] This design allowed prodrug **47** to be reduced to an active Pt(II) drug within cells while simultaneously releasing the apoptosis sensor TPS-DEVD. The reduced Pt(II) drug induced apoptosis in cancer cells and activated caspase-3. The activated caspase-3 subsequently cleaved the DEVD sequence of the apoptosis sensor and triggered the AIE effect of TPS residue, ultimately leading to fluorescence enhancement. This research presents a fluorescent probe capable of tracking the reduction of Pt(IV) complexes and evaluating the therapeutic responses.

3.5.2 Fluorophores at the position of non-leaving group. In addition to introducing fluorophores to axial positions, fluorophores can also be incorporated into the equatorial positions of Pt(IV) complexes to measure Pt(IV) reduction. Lippard and Wilson functionalized the dangling carboxylic acid moiety in a Pt(II) complex [Pt(edma)Cl_2] (edma = ethylenediaminemonoacetic acid) with dansyl ethylenediamine (Ds-en), yielding an

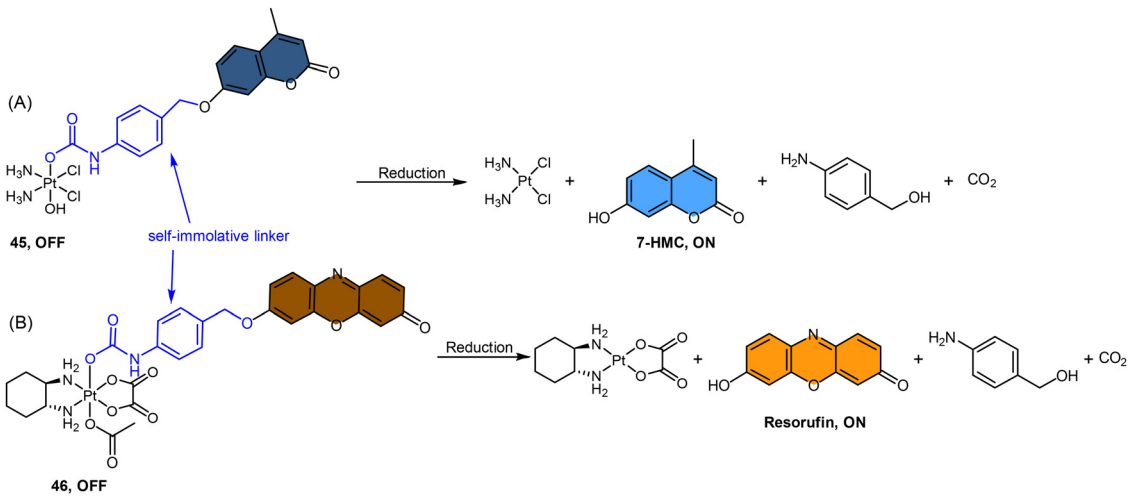

Scheme 10 The Pt(IV) complexes with axial (A) 7-HMC ligand (**45**) and (B) resorufin ligand (**46**) exhibit fluorescence 'turn-on' following the reduction of Pt(IV) complexes and release of the axial fluorophore.

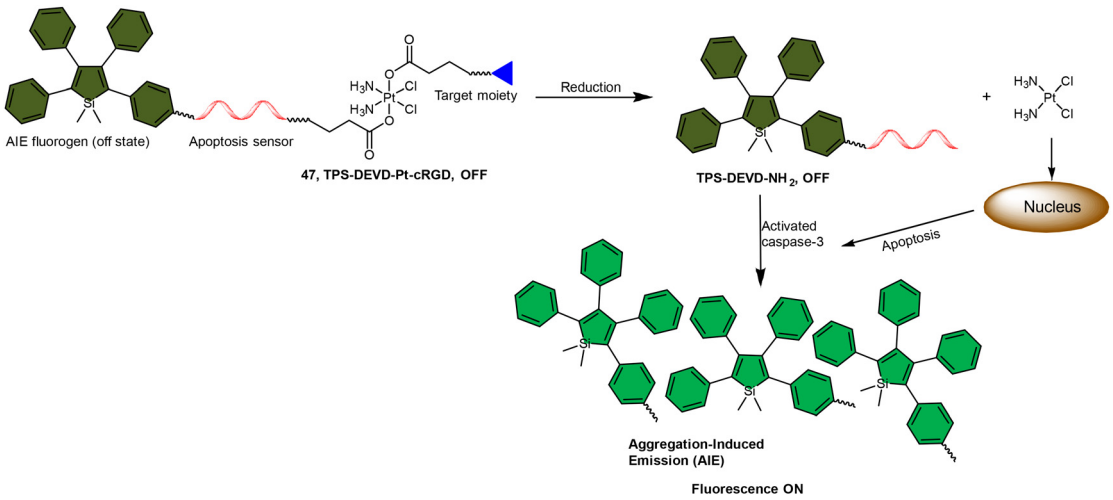

Scheme 11 Illustration of the targeted theranostic Pt(IV) prodrug **47** with a built-in aggregation-induced emission (AIE) light-up apoptosis sensor for noninvasive *in situ* early evaluation of its therapeutic responses.

intermediate **48-1**. Upon conjugation, the emission of Ds-en was slightly quenched, and the quantum yield dropped from 40% for free Ds-en to 27% for **48-1**. This intermediate underwent oxidation to afford a Pt(IV) complex **48** (Scheme 12A).[158] During the oxidation of Pt(II) to Pt(IV), the emission quantum yield decreased further from 27% for complex **48-1** to 1.6% for complex **48**. This significant decrease in emission efficiency suggested that the Pt(IV) center in **48** was more potent at quenching the dansyl-based fluorescence than the Pt(II) center in **48-1**. When complex **48** was treated with the biologically relevant reducing agent glutathione, a 6.3-fold increase in fluorescence was observed. Although employing the Pt(IV) complexes that bear fluorophores at the equatorial positions to monitor Pt(IV) reduction was only confirmed in buffers, this strategy provides useful guidance and holds promise for imaging the reduction of Pt(IV) complexes in living systems.

In another study by Hambley *et al.*, coumarin dyes were incorporated into the non-leaving position of Pt(IV) complexes (Scheme 12B).[152] Coordination of coumarin 120 (C120) at the non-leaving position of a Pt(II) drug afforded *c*-[$PtCl_2$(C120)(NH_3)] (complex **49-1**), which resulted in partial quenching of fluorescence, with a 2.5-fold decrease observed. Oxidation of complex **49-1** to its Pt(IV) form (*c*,*t*,*c*-[$PtCl_2(OH)_2$(C120)(NH_3)], complex **49**) resulted in a further 7-fold decrease in fluorescence. When complex **49** was treated with the cellular reductant ascorbate for over 2 days, it underwent reduction to form complex **49-1**. During this reduction process, a slight but steady increase in fluorescence was observed. The observed slow increment in fluorescence indicates a sluggish reduction process of the Pt(IV) complex **49**, implying its resistance to reduction in the medium prior to cellular uptake.

These coordination-sensitive fluorescent probes can serve as valuable tools for studying the cellular metabolism of plati-

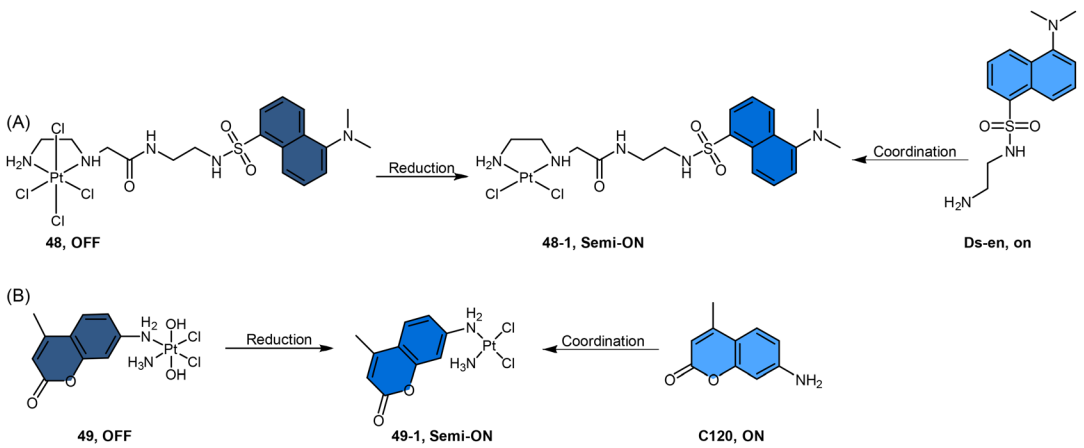

Scheme 12 The Pt(IV) complexes with non-leaving group (A) dansyl ethylenediamine (Ds-en) **48** and (B) coumarin 120 (C120) **49** exhibit fluorescence 'turn-on' following reduction of Pt(IV) complexes and a decrease in the quenching of the fluorophore.

num complexes. These probes take advantage of the fact that free fluorophores show robust fluorescence, which can be partially quenched when conjugated in the non-leaving-group position of Pt(II) complexes and be further quenched upon oxidation to Pt(IV) complexes. In this way, the regeneration of fluorescence would reflect that the reduction of Pt(IV) complexes had occurred. The fluorophores exhibited remarkable stability when conjugated to the non-leaving positions of Pt drugs. Any potential loss of these fluorophores in the reduction environments was negligible in comparison to the reduction products. Hence, this strategy can be employed specifically to monitor the reduction of the Pt(IV) complex. The changes in fluorescence induced by changes in oxidation state can be utilized to obtain information about the oxidation or coordination state of platinum complexes.

3.5.3 Fluorophores independent from the Pt scaffold. The modification of Pt(IV) complexes with bulky organic fluorophores may change the pharmacophore and alter their uptake characteristics, thus rendering distinct bioactivities compared to Pt(II) drugs. To address these limitations, Ang and Montagner developed a novel imaging probe that was independent of the Pt scaffold and could selectively interact with Pt(II) species using a recognition motif comprised of diethyldithiocarbamate (DDTC). The binding of DDTC to cisplatin would turn on the fluorescence of a rhodamine (Rho)-based dye (Scheme 13A).[86] This imaging probe was designed to be exclusively activated by Pt(II) drugs, enabling it to distinguish between Pt(IV) prodrugs and their Pt(II) congeners. Besides, the probe is exclusively effective on Pt(II) complexes that feature diam(m)ineplatinum(II) pharmacophores. The DDTC motif

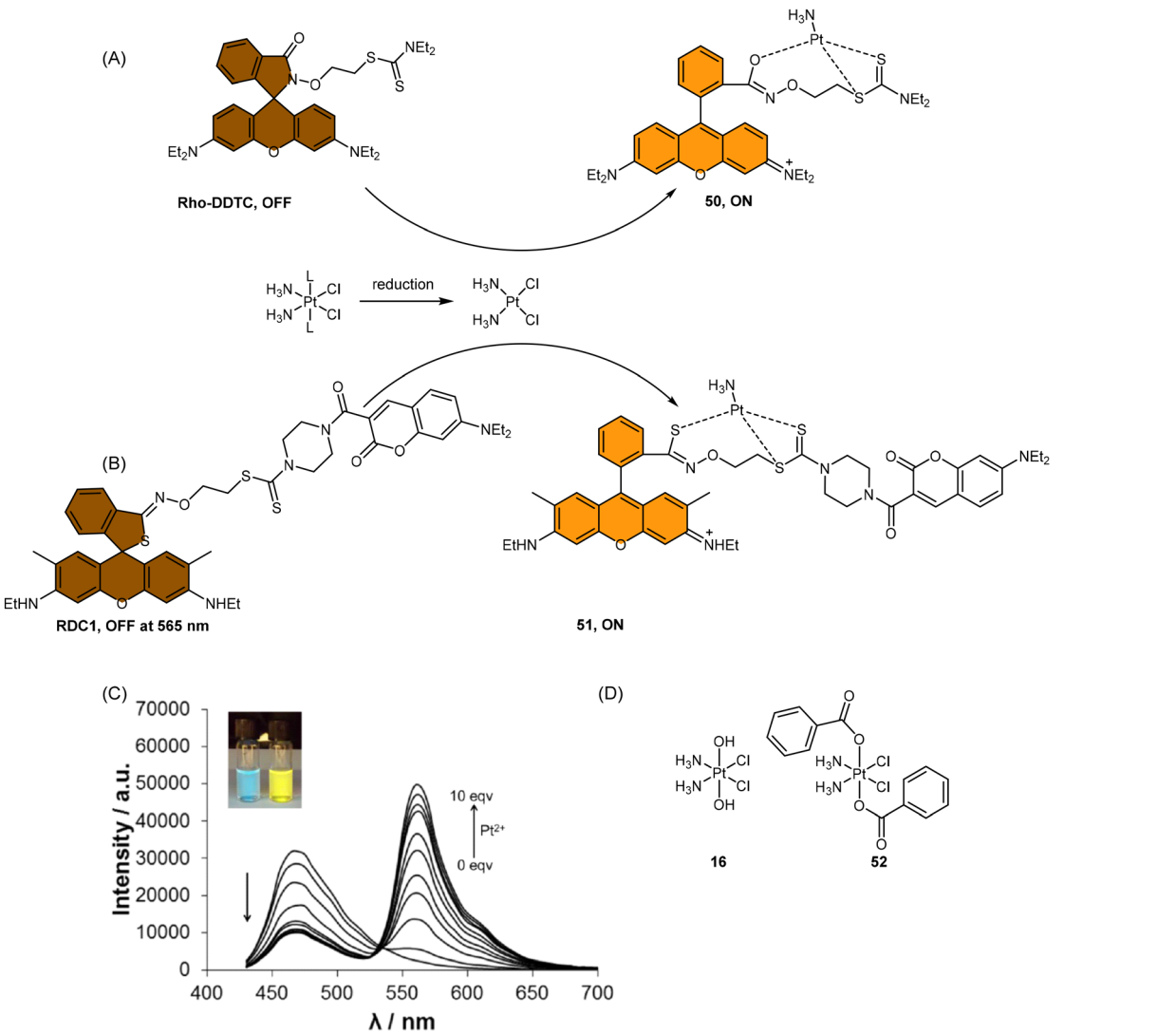

Scheme 13 (A) Proposed activation pathway of Rho-DDTC by Pt(II) complexes in the absence of aquation. (B) The FRET probe for the ratiometric sensing of cisplatin. (C) Fluorescence titration spectra of RDC1 (20 μM) in response to Pt^{2+} (0–10 eq.) in CH_3CN/HEPES buffer (v/v = 7 : 3, 5 mM, pH 7.4) (λ_{ex} = 400 nm). Inset: Change in fluorescence under irradiation by 365 nm UV lamp. Adapted with permission from ref. 85. Copyright 2018, Wiley Online Library. (D) The chemical structures of complexes **16** and **52**.

binds smoothly to cisplatin due to the low steric hindrance from the two ammine ligands in cisplatin. Moreover, the displacement of an am(m)ine ligand, which is a prerequisite for the activation of **Rho-DDTC**, is favorable in cisplatin since the ammine ligands make cisplatin kinetically unstable. For oxaliplatin that contains a chelating DACH ligand, which imparts

Table 3 Summary of the advantages, disadvantages, and applications of fluorescent probes. The color for each probe is assigned based on its respective emission wavelength

Fluorescent probes	Advantages	Disadvantages	Applications
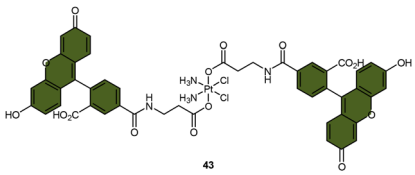 43	Monitoring cellular uptake and conversion of Pt(IV) to Pt(II)	Not able to quantify the exact amount of Pt(IV) complexes reduced	Imaging localization and reduction of Pt(IV) complex **43** in HeLa cells[114]
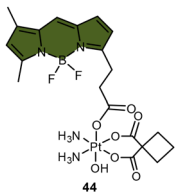 44	Monitoring the reduction of Pt(IV) prodrugs in a real-time mode	Only works well in buffer solution and cell lysate	Proteins with high molecular weights contribute more to the reduction of the Pt(IV) complex in cell lysates[83]
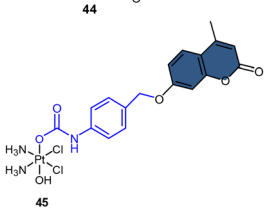 45	Propose a novel method to tether fluorophore to Pt(IV) complexes	Only investigated in a buffer solution	Tether fluorophore without carboxylate to Pt(IV) complexes[84]
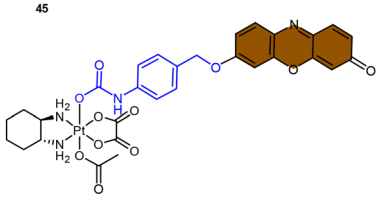 46	Monitoring the reduction of Pt(IV) complexes in hypoxia conditions	Fixed cell	Be utilized as a potential hypoxia-activated prodrug[156]
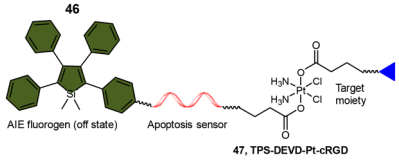 AIE fluorogen (off state) Apoptosis sensor Target moiety 47, TPS-DEVD-Pt-cRGD	Reflecting both the reduction of Pt(IV) complexes and the activated pathway	The fluorescence enhancement could not reflect the amount of Pt(IV) complexes reduced	Used as an indicator for early evaluation of the therapeutic responses[157]
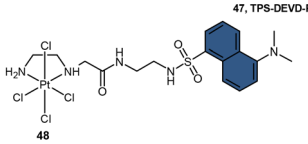 48	Monitoring the oxidation of the platinum center	Only investigated in a buffer solution	Providing new directions for imaging the reduction of Pt(IV) complexes[158]
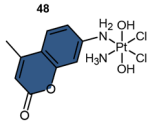 49	Monitoring the reduction	The distinction between the Pt(II) and Pt(IV) states is unclear	The probe could give information about coordination or oxidation state[152]
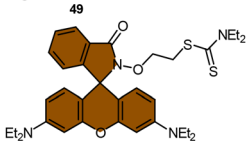 Rho-DDTC	Be able to distinguish Pt(II) and Pt(IV) complexes	(1) The fluorescence of the probe is affected by various factors (2) Fixed cell only	Imaging of cisplatin and several Pt(IV) prodrugs in HeLa cells[86]
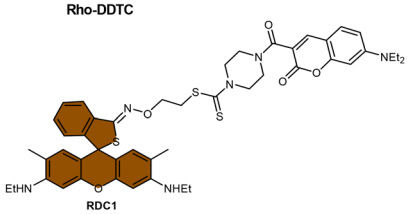 RDC1	Be able to distinguish cisplatin from its Pt(IV) counterparts	Fixed cell only	The probe could figure out that GSH is not the dominant cellular reductant of Pt(IV) complexes[85]

greater kinetic stability, probe activation was not observed. The developed probe was also used to demonstrate the intracellular reduction of a series of carboxylato Pt(IV) prodrugs in fixed cells. However, the reduction of Pt(IV) complexes and the subsequent "turn on" of fluorescence are affected by variations in probe concentrations, excitation intensities, and complex cellular environments. These factors present challenges in accurately assessing the extent of Pt(IV) complex reduction.

To address the aforementioned limitations and gain a deeper understanding of how Pt(IV) drugs are processed at the cellular level, Ang *et al.* developed a ratiometric probe **RDC1** to detect cisplatin quantitively. This probe was utilized to investigate the fate of Pt(IV) prodrugs in a cellular environment (Scheme 13B).[85] In the absence of Pt(II) compounds, the maximum emission of **RDC1** was observed at a wavelength of 470 nm; upon interaction with Pt(II) species, the fluorescence intensity at 470 nm decreased while concomitant increased at 565 nm (Scheme 13C). The ratio of emission intensities (I_{565}/I_{470}) increased from 0.07 to 4.8 in the presence of Pt(II) compound, indicating a 68-fold enhancement. Hence, the ratio of fluorescence intensities (I_{565}/I_{470}), referred to as R_{red} (reduction ratio), is a reliable measurement for quantifying the reduced Pt(IV) complex. The ratiometric probe demonstrated a notably higher R_{red} value of 0.54 for complex **52**, in contrast to 0.14 for complex **16** (Scheme 13D), showing that the ratiometric probe could quantitively determine the amount of Pt(IV) complex reduced. Furthermore, to gain deeper insights into the intracellular activation of Pt(IV) prodrugs, the authors conducted a study to examine the role of the cellular reductant GSH in the activation process utilizing the ratiometric probe. The results revealed that the reduction of complex **52** in GSH-depleted cells was similar to that in GSH-normal cells, suggesting that GSH may not be the dominant cellular reductant for Pt(IV) complexes. Although the ratiometric probe **RDC1** has proven to be a reliable means for quantitatively detecting cisplatin and exploring the role of GSH in reducing Pt(IV) prodrugs in a cellular context, its usage necessitates the fixation of cells with paraformaldehyde, probably due to the probe's slow reaction kinetics, which prevents the real-time monitoring the activation of Pt(IV) prodrugs in live cells.

In general, fluorescence spectroscopy is a widely employed technique to monitor the activation of Pt(IV) complexes by observing the subsequent fluorescence turn-on during reduction reactions (Table 3). The high sensitivity of fluorescence spectroscopy enables researchers to track the reduction of Pt(IV) complexes, even at minimal concentrations. Furthermore, this technique provides valuable spatial information by enabling the observation of the uptake, distribution, and localization of Pt(IV) complexes, as well as their reduction process within cells or specific regions of interest. Fluorescent Pt(IV) probes that can enter cells have been particularly useful for real-time monitoring of their distribution and dynamic processes using fluorescence spectroscopy. However, accurately quantifying the amount of Pt(IV) complex reduced has proven

Table 4 The summary of techniques used to monitor the reduction of Pt(IV) complexes

Detection techniques	Advantages	Disadvantages	Applications
UV-Vis spectroscopy	The method is sensitive and easy to perform	This approach does not provide any information on the identity of the reduction products Due to the high background in cells, it cannot be used to monitor the reduction of the Pt(IV) complexes in live cells	It can be applied to monitor the reduction of Pt(IV) without other chromophores that absorb in the same region
HPLC	This method could monitor the reduction of the Pt(IV) complex and the generation of Pt(II) species and the released ligands, whose identity could also be identified by retention time	HPLC requires solution-based samples, making it unsuitable for monitoring the reduction of Pt(IV) complex in live cells	HPLC analysis is the current gold standard for evaluating Pt(IV) reduction
XANES	The method could monitor the oxidation change of the platinum center	Requiring sophisticated sample preparation, including collecting and freezing cells, this technique fails to monitor the reduction of Pt(IV) prodrugs neither in live cells nor in a real-time mode	The reduction of Pt(IV) complexes in the biological environment could be observed by measuring the relative proportions of two different oxidation states of both Pt(II) and Pt(IV)
NMR spectroscopy	Providing sufficient information about the oxidation state and coordination environment of platinum, as well as reduction products	High concentration demanded; low sensitivity	Different types of NMR were used for the situations and research purposes to efficiently monitor the reduction of the Pt(IV) complex
Fluorescence spectroscopy	Providing good resolution to identify the uptake, colocalization, and reduction of Pt(IV) complex	Noninvasive fluorescence imaging needs excitation light, which can lead to tissue auto-fluorescence and cell damage The fluorescence can be vigorously quenched by tissue components and influenced by various factors, leading to a high background	Fluorescence spectroscopy has been widely used to study the reduction of Pt(IV) complexes in cells

challenging. While some probes can provide quantitative measurements of reduced Pt(IV) complexes, their efficacy is limited to fixed cells or cell lysate and not applicable to live cells. Therefore, there is a demand for fluorescent Pt(IV) probes that can enter live cells and allow investigation of their cellular processing. Furthermore, the challenges associated with fluorescence spectroscopy pose an additional obstacle to accurately quantifying the activation of Pt(IV) complexes within cells. The fluorophores used to monitor the activation of the Pt(IV) complex by fluorescence spectroscopy may undergo photobleaching, which leads to a decrease in fluorescence signal over time, limiting the duration of imaging experiments and affecting the accuracy of long-term observations.[159] Moreover, noninvasive fluorescence imaging requires excitation light, and continuous exposure to such excitation light, especially at short wavelengths, may induce cellular damage and interfere with biological processes.

4. Conclusions and perspectives

The reduction of Pt(IV) complexes could be monitored by various techniques (Table 4), each technique with its own advantages and limitations. UV spectroscopy is a convenient and easily accessible technique for monitoring Pt(IV) reduction processes and is comparatively more straightforward than other analytical techniques. However, it is not capable of identifying the specific reduction products and is not suitable for monitoring Pt(IV) reduction in live cells where there is a high background. HPLC is a reliable technique for analyzing and quantifying the reduction of Pt(IV) complexes, as well as the generation of Pt(II) species and the released ligands. The identity of these reduction products can be determined by their characteristic retention time; their identity can also be verified through electrospray ionization (ESI) mass and liquid chromatography-mass spectrometry (LC-MS) techniques.[62,84,114–116] HPLC is also valuable for time-resolved analysis, allowing for investigating reaction kinetics and tracking the reduction progress over time. However, HPLC does not provide real-time monitoring and requires batch-wise analysis, which may not capture rapid changes or transient species during the reduction process. XANES is a powerful technique for detecting variations in the oxidation state of the platinum center, and it can provide quantitative information about the relative concentrations of different Pt states present in the cells. However, sample preparation for XANES analysis is complicated, time-consuming, and technically demanding. It is not suitable for real-time or live-cell monitoring of Pt(IV) prodrug reduction. Moreover, access to synchrotron radiation facilities is required for high-energy X-ray measurements using XANES, which may pose logistic challenges. NMR spectroscopy is an indispensable analytical tool in examining the activation of Pt(IV) complexes, providing detailed information about the oxidation state and coordination environment of Pt, and facilitating the identification and characterization of reduction products. Furthermore, it is a non-destructive technique, allowing for the recovery of samples for further analysis. However, NMR spectroscopy may face challenges related to low sensitivity, especially with low concentrations of Pt species or rapid reaction kinetics. In such cases, longer acquisition times or higher concentrations of the Pt(IV) complex may be required, respectively, to achieve adequate sensitivity and high signal-to-noise ratios. Fluorescence spectroscopy provides high resolution to identify the uptake, colocalization, and reduction of Pt(IV) complex within cells. Nevertheless, the use of fluorophores in fluorescence spectroscopy for monitoring the activation of the Pt(IV) complex can be limited by photobleaching, which may compromise the accuracy of long-term observations. Furthermore, noninvasive fluorescence imaging necessitates excitation light, and prolonged exposure to high-intensity light carries the inherent risk of inducing phototoxicity in cellular systems.[159–161]

Generally, the strategies applied in buffer systems, such as UV, HPLC, and NMR, provide sufficient information about the time scale of the reduction event and the identities of the reduction products. To evaluate the reduction of a novel Pt(IV) complex, HPLC analysis usually serves as the gold standard if the complex can be detected by the HPLC instrument and exhibits a distinguishable retention time on the column. The highly sensitive nature of HPLC allows for the measurement of the reduction rate of and identification of reduction products using only trace amounts of the complex (in μM). In cases where the Pt(IV) complex's retention time overlaps with the dead volume on the HPLC column, but distinct absorption bands are still observed in the UV-Vis spectrum, UV-Vis spectroscopy can be employed to monitor the reduction process. If a more in-depth analysis of the reduction of Pt(IV) complexes at the cellular level is required, researchers can utilize techniques such as XANES, ^{19}F NMR, and fluorescence spectroscopy. These methods provide valuable insights into the role of biological reductants and ligands located at axial or equatorial positions in the reduction process.

In conclusion, Pt(IV) prodrugs have emerged as highly promising candidates as next-generation anticancer drugs. The effectiveness of these prodrugs in combating cancers heavily depends on their reduction profile, both in buffer solutions and, more importantly, within cells. Tracking the reduction process of various Pt(IV) complexes using different techniques can help anticipate and even improve the anticancer efficiency of these complexes. This review serves as a comprehensive resource for researchers aiming to stay updated on the latest advancements in strategies used to monitor the reduction, learn from exemplary research, and contribute to the mechanistic understanding of metal-based drugs in cellular and even *in vivo* contexts. Since current techniques have some limitations, it is necessary to develop novel strategies capable of real-time monitoring of Pt(IV) reduction in live cells and uncover the mechanisms and timing of the reduction process, including the exact roles of reducing agents. These advancements hold great potential in elucidating the intrinsic mechanisms involved in Pt(IV) prodrug activation in live cells and *in vivo*, thus providing invaluable insights for the rational design of novel Pt(IV) prodrugs.

Conflicts of interest

There are no conflicts to declare.

Acknowledgements

We thank the National Natural Science Foundation of China (Grant No. 22077108 and 22277103), the Hong Kong Research Grants Council (Grant No. CityU 11303320, 11302221, 11313222, and 11304923), the Science Technology and Innovation Committee of Shenzhen Municipality (JCYJ20210324120004011), and the City University of Hong Kong (Grant No. 7020014) for funding support.

References

1 R. A. Alderden, M. D. Hall and T. W. Hambley, The discovery and development of cisplatin, *J. Chem. Educ.*, 2006, **83**, 728.
2 S. Ghosh, Cisplatin: the first metal based anticancer drug, *Bioorg. Chem.*, 2019, **88**, 102925.
3 J. J. Wilson and S. J. Lippard, Synthetic methods for the preparation of platinum anticancer complexes, *Chem. Rev.*, 2014, **114**, 4470–4495.
4 B. Rosenberg, L. Van Camp and T. Krigas, Inhibition of cell division in *Escherichia coli*, by electrolysis products from a platinum electrode, *Nature*, 1965, **205**, 698–699.
5 S. Dasari and P. B. Tchounwou, Cisplatin in cancer therapy: molecular mechanisms of action, *Eur. J. Pharmacol.*, 2014, **740**, 364–378.
6 I. Kostova, Platinum complexes as anticancer agents, *Recent Pat. Anticancer Drug Discovery*, 2006, **1**, 1–22.
7 W. J. van der Vijgh, Clinical pharmacokinetics of carboplatin, *Clin. Pharmacokinet.*, 1991, **21**, 242–261.
8 H. Calvert, The clinical development of carboplatin – A personal perspective, *Inorg. Chim. Acta*, 2019, **498**, 118987.
9 A. M. Di Francesco, A. Ruggiero and R. Riccardi, Cellular and molecular aspects of drugs of the future: oxaliplatin, *Cell. Mol. Life Sci.*, 2002, **59**, 1914–1927.
10 E. Raymond, S. G. Chaney, A. Taamma and E. Cvitkovic, Oxaliplatin: a review of preclinical and clinical studies, *Ann. Oncol.*, 1998, **9**, 1053–1071.
11 T. C. Johnstone, K. Suntharalingam and S. J. Lippard, The next generation of platinum drugs: targeted Pt(II) agents, nanoparticle delivery, and Pt(IV) prodrugs, *Chem. Rev.*, 2016, **116**, 3436–3486.
12 L. Kelland, The resurgence of platinum-based cancer chemotherapy, *Nat. Rev. Cancer*, 2007, **7**, 573–584.
13 N. J. Wheate, S. Walker, G. E. Craig and R. Oun, The status of platinum anticancer drugs in the clinic and in clinical trials, *Dalton Trans.*, 2010, **39**, 8113–8127.
14 E. R. Jamieson and S. J. Lippard, Structure, recognition, and processing of cisplatin–DNA adducts, *Chem. Rev.*, 1999, **99**, 2467–2498.
15 J. Reedijk, Why does cisplatin reach guanine-N7 with competing S-donor ligands available in the cell?, *Chem. Rev.*, 1999, **99**, 2499–2510.
16 B. W. Harper, A. M. Krause-Heuer, M. P. Grant, M. Manohar, K. B. Garbutcheon-Singh and J. R. Aldrich-Wright, Advances in platinum chemotherapeutics, *Chem. – Eur. J.*, 2010, **16**, 7064–7077.
17 R. Oun, Y. E. Moussa and N. J. Wheate, The side effects of platinum-based chemotherapy drugs: a review for chemists, *Dalton Trans.*, 2018, **47**, 6645–6653.
18 J. T. Hartmann and H.-P. Lipp, Toxicity of platinum compounds, *Expert Opin. Pharmacother.*, 2003, **4**, 889–901.
19 Z. H. Siddik, Cisplatin: mode of cytotoxic action and molecular basis of resistance, *Oncogene*, 2003, **22**, 7265–7279.
20 A.-M. Florea and D. Büsselberg, Cisplatin as an antitumor drug: cellular mechanisms of activity, drug resistance and induced side effects, *Cancers*, 2011, **3**, 1351–1371.
21 J. J. Wilson and S. J. Lippard, Synthesis, characterization, and cytotoxicity of platinum(IV) carbamate complexes, *Inorg. Chem.*, 2011, **50**, 3103–3115.
22 E. Wexselblatt and D. Gibson, What do we know about the reduction of Pt(IV) pro-drugs?, *J. Inorg. Biochem.*, 2012, **117**, 220–229.
23 C. K. J. Chen and T. W. Hambley, The impact of highly electron withdrawing carboxylato ligands on the stability and activity of platinum(IV) pro-drugs, *Inorg. Chim. Acta*, 2019, **494**, 84–90.
24 S. Chen, H. Yao, Q. Zhou, M.-K. Tse, Y. F. Gunawan and G. Zhu, Stability, reduction, and cytotoxicity of platinum (IV) anticancer prodrugs bearing carbamate axial ligands: comparison with their carboxylate analogues, *Inorg. Chem.*, 2020, **59**, 11676–11687.
25 Z. Li, X.-J. Ding, X. Qiao, X.-M. Liu, X. Qiao, C.-Z. Xie, R.-P. Liu and J.-Y. Xu, Thalidomide-based Pt(IV) prodrugs designed to exert synergistic effect of immunomodulation and chemotherapy, *J. Inorg. Biochem.*, 2022, **232**, 111842.
26 X.-M. Liu, Z. Li, X.-R. He, R.-P. Liu, Z.-Y. Ma, X. Qiao, S.-Q. Wang and J.-Y. Xu, Dual-targeting of the aromatase binding domain of heme and androstenedione by Pt(IV) prodrugs: a new treatment for postmenopausal breast cancer, *Inorg. Chem. Front.*, 2022, **9**, 3470–3483.
27 S. Dhar, Z. Liu, J. Thomale, H. Dai and S. J. Lippard, Targeted single-wall carbon nanotube-mediated Pt(IV) prodrug delivery using folate as a homing device, *J. Am. Chem. Soc.*, 2008, **130**, 11467–11476.
28 L. Ma, R. Ma, Y. Wang, X. Zhu, J. Zhang, H. C. Chan, X. Chen, W. Zhang, S.-K. Chiu and G. Zhu, Chalcoplatin, a dual-targeting and p53 activator-containing anticancer platinum(IV) prodrug with unique mode of action, *Chem. Commun.*, 2015, **51**, 6301–6304.
29 N. Muhammad, N. Sadia, C. Zhu, C. Luo, Z. Guo and X. Wang, Biotin-tagged platinum(IV) complexes as targeted cytostatic agents against breast cancer cells, *Chem. Commun.*, 2017, **53**, 9971–9974.
30 M. Srinivasarao and P. S. Low, Ligand-targeted drug delivery, *Chem. Rev.*, 2017, **117**, 12133–12164.

31 S. Dhar and S. J. Lippard, Mitaplatin, a potent fusion of cisplatin and the orphan drug dichloroacetate, *Proc. Natl. Acad. Sci. U. S. A.*, 2009, **106**, 22199–22204.
32 D. Gibson, Platinum(IV) anticancer agents; are we en route to the holy grail or to a dead end?, *J. Inorg. Biochem.*, 2021, **217**, 111353.
33 W. H. Ang, I. Khalaila, C. S. Allardyce, L. Juillerat-Jeanneret and P. J. Dyson, Rational design of platinum(IV) compounds to overcome glutathione-S-transferase mediated drug resistance, *J. Am. Chem. Soc.*, 2005, **127**, 1382–1383.
34 Q. Chen, Y. Yang, X. Lin, W. Ma, G. Chen, W. Li, X. Wang and Z. Yu, Platinum(IV) prodrugs with long lipid chains for drug delivery and overcoming cisplatin resistance, *Chem. Commun.*, 2018, **54**, 5369–5372.
35 Z. Xu, Z. Wang, Z. Deng and G. Zhu, Recent advances in the synthesis, stability, and activation of platinum(IV) anticancer prodrugs, *Coord. Chem. Rev.*, 2021, **442**, 213991.
36 M. D. Hall and T. W. Hambley, Platinum(IV) antitumour compounds: their bioinorganic chemistry, *Coord. Chem. Rev.*, 2002, **232**, 49–67.
37 A. Nemirovski, I. Vinograd, K. Takrouri, A. Mijovilovich, A. Rompel and D. Gibson, New reduction pathways for *ctc*-$[PtCl_2(CH_3CO_2)_2(NH_3)(Am)]$ anticancer prodrugs, *Chem. Commun.*, 2010, **46**, 1842–1844.
38 Q. Zhou, S. Chen, Z. Xu, G. Liu, S. Zhang, Z. Wang, M. K. Tse, S. M. Yiu and G. Zhu, Multitargeted platinum (IV) anticancer complexes bearing pyridinyl ligands as axial leaving groups, *Angew. Chem., Int. Ed.*, 2023, **62**, e202302156.
39 T. Yempala, T. Babu, S. Karmakar, A. Nemirovski, M. Ishan, V. Gandin and D. Gibson, Expanding the arsenal of Pt^{IV} anticancer agents: multi–action Pt^{IV} anticancer agents with bioactive ligands possessing a hydroxy functional group, *Angew. Chem., Int. Ed.*, 2019, **58**, 18218–18223.
40 S. Chen, K.-Y. Ng, Q. Zhou, H. Yao, Z. Deng, M.-K. Tse and G. Zhu, The influence of different carbonate ligands on the hydrolytic stability and reduction of platinum(IV) prodrugs, *Dalton Trans.*, 2022, **51**, 885–897.
41 S. Choi, C. Filotto, M. Bisanzo, S. Delaney, D. Lagasee, J. L. Whitworth, A. Jusko, C. Li, N. A. Wood, J. Willingham, A. Schwenker and K. Spaulding, Reduction and anticancer activity of platinum(IV) complexes, *Inorg. Chem.*, 1998, **37**, 2500–2504.
42 C. K. J. Chen, P. Kappen and T. W. Hambley, The reduction of *cis*-platinum(IV) complexes by ascorbate and in whole human blood models using ^{1}H NMR and XANES spectroscopy, *Metallomics*, 2019, **11**, 686–695.
43 Y. Liu, H. Tian, L. Xu, L. Zhou, J. Wang, B. Xu, C. Liu, L. I. Elding and T. Shi, Investigations of the kinetics and mechanism of reduction of a carboplatin Pt(IV) prodrug by the major small-molecule reductants in human plasma, *Int. J. Mol. Sci.*, 2019, **20**, 5660.
44 J. Dong, Y. Ren, S. Huo, S. Shen, J. Xu, H. Tian and T. Shi, Reduction of ormaplatin and *cis*-diamminetetrachloroplatinum(IV) by ascorbic acid and dominant thiols in human plasma: kinetic and mechanistic analyses, *Dalton Trans.*, 2016, **45**, 11326–11337.
45 K. Lemma, J. Berglund, N. Farrell and L. I. Elding, Kinetics and mechanism for reduction of anticancer-active tetrachloroam(m)ine platinum(IV) compounds by glutathione, *J. Biol. Inorg. Chem.*, 2000, **5**, 300–306.
46 V. Pichler, P. Heffeter, S. M. Valiahdi, C. R. Kowol, A. Egger, W. Berger, M. A. Jakupec, M. S. Galanski and B. K. Keppler, Unsymmetric mono- and dinuclear platinum(IV) complexes featuring an ethylene glycol moiety: synthesis, characterization, and biological activity, *J. Med. Chem.*, 2012, **55**, 11052–11061.
47 V. Pichler, S. Göschl, E. Schreiber-Brynzak, M. A. Jakupec, M. S. Galanski and B. K. Keppler, Influence of reducing agents on the cytotoxic activity of platinum(IV) complexes: induction of G_2/M arrest, apoptosis and oxidative stress in A2780 and cisplatin resistant A2780cis cell lines, *Metallomics*, 2015, **7**, 1078–1090.
48 T. J. O'Rourke, G. R. Weiss, P. New, H. A. Burris III, G. Rodriguez, J. Eckhardt, J. Hardy, J. G. Kuhn, S. Fields, G. M. Clark and D. D. Von Hoff, Phase I clinical trial of ormaplatin (tetraplatin, NSC 363812), *Anti-Cancer Drugs*, 1994, **5**, 520–526.
49 Y. Shi, S.-A. Liu, D. J. Kerwood, J. Goodisman and J. C. Dabrowiak, Pt(IV) complexes as prodrugs for cisplatin, *J. Inorg. Biochem.*, 2012, **107**, 6–14.
50 L. Pendyala, J. W. Cowens, G. B. Chheda, S. P. Dutta and P. J. Creaven, Identification of *cis*-dichloro-bis-isopropylamine platinum(II) as a major metabolite of iproplatin in humans, *Cancer Res.*, 1988, **48**, 3533–3536.
51 V. H. Bramwell, D. Crowther, S. O'Malley, R. Swindell, R. Johnson, E. H. Cooper, N. Thatcher and A. Howell, Activity of JM9 in advanced ovarian cancer: a phase I-II trial, *Cancer Treat. Rep.*, 1985, **69**, 409–416.
52 L. R. Kelland, An update on satraplatin: the first orally available platinum anticancer drug, *Expert Opin. Invest. Drugs*, 2000, **9**, 1373–1382.
53 N. Graf and S. J. Lippard, Redox activation of metal-based prodrugs as a strategy for drug delivery, *Adv. Drug Delivery Rev.*, 2012, **64**, 993–1004.
54 M. D. Hall, H. R. Mellor, R. Callaghan and T. W. Hambley, Basis for design and development of platinum(IV) anticancer complexes, *J. Med. Chem.*, 2007, **50**, 3403–3411.
55 P. Sova, A. Mistr, A. Kroutil, F. Zak, P. Pouckova and M. Zadinova, Preclinical anti-tumor activity of a new oral platinum(IV) drug LA-12, *Anti-Cancer Drugs*, 2005, **16**, 653–657.
56 V. Kvardova, R. Hrstka, D. Walerych, P. Muller, E. Matoulkova, V. Hruskova, D. Stelclova, P. Sova and B. Vojtesek, The new platinum(IV) derivative LA-12 shows stronger inhibitory effect on Hsp90 function compared to cisplatin, *Mol. Cancer*, 2010, **9**, 1–9.
57 D. Gibson, Platinum(IV) anticancer prodrugs – hypotheses and facts, *Dalton Trans.*, 2016, **45**, 12983–12991.
58 J. R. Gispert, *Coordination chemistry*, Wiley-VCH Weinheim, 2008.

59 G. L. Miessler, *Inorganic chemistry*, Pearson Education India, 2008.
60 T. C. Johnstone, S. M. Alexander, J. J. Wilson and S. J. Lippard, Oxidative halogenation of cisplatin and carboplatin: synthesis, spectroscopy, and crystal and molecular structures of Pt(IV) prodrugs, *Dalton Trans.*, 2015, **44**, 119–129.
61 X. Hu, F. Li, N. Noor and D. Ling, Platinum drugs: from Pt(II) compounds, Pt(IV) prodrugs, to Pt nanocrystals/nanoclusters, *Sci. Bull.*, 2017, **62**, 589–596.
62 H. Shi, C. Imberti and P. J. Sadler, Diazido platinum(IV) complexes for photoactivated anticancer chemotherapy, *Inorg. Chem. Front.*, 2019, **6**, 1623–1638.
63 F. S. Mackay, J. A. Woods, H. Moseley, J. Ferguson, A. Dawson, S. Parsons and P. J. Sadler, A photoactivated trans–diammine platinum complex as cytotoxic as cisplatin, *Chem. – Eur. J.*, 2006, **12**, 3155–3161.
64 N. J. Farrer, J. A. Woods, L. Salassa, Y. Zhao, K. S. Robinson, G. J. Clarkson, F. S. Mackay and P. J. Sadler, A potent *trans*-diimine platinum anticancer complex photoactivated by visible light, *Angew. Chem., Int. Ed.*, 2010, **49**, 8905–8908.
65 H.-C. Tai, Y. Zhao, N. J. Farrer, A. E. Anastasi, G. Clarkson, P. J. Sadler and R. J. Deeth, A computational approach to tuning the photochemistry of platinum(IV) anticancer agents, *Chem. – Eur. J.*, 2012, **18**, 10630–10642.
66 J. A. Platts, S. P. Oldfield, M. M. Reif, A. Palmucci, E. Gabano and D. Osella, The RP-HPLC measurement and QSPR analysis of $\log P_{o/w}$ values of several Pt(II) complexes, *J. Inorg. Biochem.*, 2006, **100**, 1199–1207.
67 S. D. Kumar and D. R. H. Kumar, Importance of RP-HPLC in analytical method development: a review, *Int. J. Pharma Sci. Res.*, 2012, **3**, 4626–4633.
68 S. Jovanović, B. Petrović and Ž. D. Bugarčić, UV-Vis, HPLC, and ^{1}H-NMR studies of the substitution reactions of some Pt(IV) complexes with 5′-GMP and L-histidine, *J. Coord. Chem.*, 2010, **63**, 2419–2430.
69 T. Niu, W. Wan, X. Li, D. Su, S. Huo and S. Shen, Reduction of platinum(IV) prodrug model complex *trans*-$[PtCl_2(CN)_4]^{2-}$ by a peptide containing cysteine and methionine groups: HPLC and MS studies, *J. Mol. Liq.*, 2018, **252**, 24–29.
70 M. D. Hall, H. L. Daly, J. Z. Zhang, M. Zhang, R. A. Alderden, D. Pursche, G. J. Foran and T. W. Hambley, Quantitative measurement of the reduction of platinum(IV) complexes using X-ray absorption near-edge spectroscopy (XANES), *Metallomics*, 2012, **4**, 568–575.
71 M. D. Hall, G. J. Foran, M. Zhang, P. J. Beale and T. W. Hambley, XANES determination of the platinum oxidation state distribution in cancer cells treated with platinum(IV) anticancer agents, *J. Am. Chem. Soc.*, 2003, **125**, 7524–7525.
72 F. W. Lytle, Determination of *d*-band occupancy in pure metals and supported catalysts by measurement of the LIII X-ray absorption threshold, *J. Catal.*, 1976, **43**, 376–379.
73 B. Shelimov, J.-F. Lambert, M. Che and B. Didillon, Application of NMR to interfacial coordination chemistry: a ^{195}Pt NMR study of the interaction of hexachloroplatinic acid aqueous solutions with alumina, *J. Am. Chem. Soc.*, 1999, **121**, 545–556.
74 P. S. Pregosin, M. Kretschmer, W. Preetz and G. Rimkus, ^{195}Pt NMR studies on stereoisomeric chloro bromo platinates(IV), *Z. Naturforsch., B: Anorg. Chem., Org. Chem.*, 1982, **37**, 1422–1424.
75 B. M. Still, P. G. A. Kumar, J. R. Aldrich-Wright and W. S. Price, ^{195}Pt NMR—Theory and application, *Chem. Soc. Rev.*, 2007, **36**, 665–686.
76 J. R. L. Priqueler, I. S. Butler and F. D. Rochon, An overview of ^{195}Pt nuclear magnetic resonance spectroscopy, *Appl. Spectrosc. Rev.*, 2006, **41**, 185–226.
77 J. Z. Zhang, E. Wexselblatt, T. W. Hambley and D. Gibson, Pt(IV) analogs of oxaliplatin that do not follow the expected correlation between electrochemical reduction potential and rate of reduction by ascorbate, *Chem. Commun.*, 2012, **48**, 847–849.
78 S. Yuan, Y. Zhu, Y. Dai, Y. Wang, D. Jin, M. Liu, L. Tang, F. Arnesano, G. Natile and Y. Liu, ^{19}F NMR allows the investigation of the fate of platinum(IV) prodrugs in physiological conditions, *Angew. Chem., Int. Ed.*, 2022, **61**, e202114250.
79 Z. Xu, H. M. Chan, C. Li, Z. Wang, M.-K. Tse, Z. Tong and G. Zhu, Synthesis, structure, and cytotoxicity of oxaliplatin-based platinum(IV) anticancer prodrugs bearing one axial fluoride, *Inorg. Chem.*, 2018, **57**, 8227–8235.
80 M. Ravera, E. Gabano, I. Zanellato, F. Fregonese, G. Pelosi, J. A. Platts and D. Osella, Antiproliferative activity of a series of cisplatin-based Pt(IV)-acetylamido/carboxylato prodrugs, *Dalton Trans.*, 2016, **45**, 5300–5309.
81 J. R. Lakowicz, *Principles of fluorescence spectroscopy*, Springer US, Boston, MA, 3rd edn, 2006.
82 J. Hernando, M. van der Schaaf, E. M. H. P. van Dijk, M. Sauer, M. F. García-Parajó and N. F. van Hulst, Excitonic behavior of rhodamine dimers: a single-molecule study, *J. Phys. Chem. A*, 2003, **107**, 43–52.
83 H. Yao and G. Zhu, A platinum-based fluorescent "turn on" sensor to decipher the reduction of platinum(IV) prodrugs, *Dalton Trans.*, 2022, **51**, 5394–5398.
84 V. E. Y. Lee, Z. C. Lim, S. L. Chew and W. H. Ang, Strategy for traceless codrug delivery with platinum(IV) prodrug complexes using self-immolative linkers, *Inorg. Chem.*, 2021, **60**, 1823–1831.
85 J. X. Ong, C. S. Q. Lim, H. V. Le and W. H. Ang, A ratiometric fluorescent probe for cisplatin: investigating the intracellular reduction of platinum(IV) prodrug complexes, *Angew. Chem., Int. Ed.*, 2019, **58**, 164–167.
86 D. Montagner, S. Q. Yap and W. H. Ang, A fluorescent probe for investigating the activation of anticancer platinum(IV) prodrugs based on the cisplatin scaffold, *Angew. Chem., Int. Ed.*, 2013, **52**, 11785–11789.
87 R. G. Pearson, Chemical hardness and bond dissociation energies, *J. Am. Chem. Soc.*, 1988, **110**, 7684–7690.

88 M. Arsenijević, M. Milovanović, V. Volarević, D. Čanović, N. Arsenijević, T. Soldatović, S. Jovanović and Ž. D. Bugarčić, Cytotoxic properties of platinum(IV) and dinuclear platinum(II) complexes and their ligand substitution reactions with guanosine-5′-monophosphate, *Transition Met. Chem.*, 2012, **37**, 481–488.

89 M. Crespo, M. Font-Bardia, P. Hamidizadeh, M. Martínez and S. M. Nabavizadeh, Kinetico-mechanistic study on the reduction/complexation sequence of Pt^{IV}/Pt^{II} organometallic complexes by thiol-containing biological molecules, *Inorg. Chim. Acta*, 2019, **486**, 8–16.

90 I. Zanellato, I. Bonarrigo, D. Colangelo, E. Gabano, M. Ravera, M. Alessio and D. Osella, Biological activity of a series of cisplatin-based aliphatic bis(carboxylato) Pt(IV) prodrugs: how long the organic chain should be?, *J. Inorg. Biochem.*, 2014, **140**, 219–227.

91 N. A. Kratochwil and P. J. Bednarski, Relationships between reduction properties and cancer cell growth inhibitory activities of *cis*–dichloro– and *cis*–diiodo–Pt(IV)–ethylenediamines, *Arch. Pharm. Pharm. Med. Chem.*, 1999, **332**, 279–285.

92 K. Lemma, T. Shi and L. I. Elding, Kinetics and mechanism for reduction of the anticancer prodrug *trans*,*trans*, *trans*-$[PtCl_2(OH)_2(c,\text{-}C_6H_{11}NH_2)(NH_3)]$ (JM335) by thiols, *Inorg. Chem.*, 2000, **39**, 1728–1734.

93 N. G. Blanco, C. R. Maldonado and J. C. Mareque-Rivas, Effective photoreduction of a Pt(IV) complex with quantum dots: a feasible new light-induced method of releasing anticancer Pt(II) drugs, *Chem. Commun.*, 2009, 5257–5259.

94 S. Choi, S. Mahalingaiah, S. Delaney, N. R. Neale and S. Masood, Substitution and reduction of platinum(IV) complexes by a nucleotide, guanosine 5′-monophosphate, *Inorg. Chem.*, 1999, **38**, 1800–1805.

95 K. Lemma, A. M. Sargeson and L. I. Elding, Kinetics and mechanism for reduction of oral anticancer platinum(IV) dicarboxylate compounds by L-ascorbate ions, *Dalton Trans.*, 2000, 1167–1172.

96 F. S. Mackay, N. J. Farrer, L. Salassa, H.-C. Tai, R. J. Deeth, S. A. Moggach, P. A. Wood, S. Parsons and P. J. Sadler, Synthesis, characterisation and photochemistry of Pt^{IV} pyridyl azido acetato complexes, *Dalton Trans.*, 2009, 2315–2325.

97 Z. Wang, N. Wang, S.-C. Cheng, K. Xu, Z. Deng, S. Chen, Z. Xu, K. Xie, M.-K. Tse, P. Shi, H. Hirao, C.-C. Ko and G. Zhu, Phorbiplatin, a highly potent Pt(IV) antitumor prodrug that can be controllably activated by red light, *Chem*, 2019, **5**, 3151–3165.

98 Y. Kido, A. R. Khokhar and Z. H. Siddik, Glutathione-mediated modulation of tetraplatin activity against sensitive and resistant tumor cells, *Biochem. Pharmacol.*, 1994, **47**, 1635–1642.

99 E. L. Weaver and R. N. Bose, Platinum(II) catalysis and radical intervention in reductions of platinum(IV) antitumor drugs by ascorbic acid, *J. Inorg. Biochem.*, 2003, **95**, 231–239.

100 S. Karmakar, I. Poetsch, C. R. Kowol, P. Heffeter and D. Gibson, Synthesis and cytotoxicity of water-soluble dual- and triple-action satraplatin derivatives: replacement of equatorial chlorides of satraplatin by acetates, *Inorg. Chem.*, 2019, **58**, 16676–16688.

101 L. Ma, N. Wang, R. Ma, C. Li, Z. Xu, M. K. Tse and G. Zhu, Monochalcoplatin: an actively transported, quickly reducible, and highly potent Pt(IV) anticancer prodrug, *Angew. Chem., Int. Ed.*, 2018, **57**, 9098–9102.

102 Z. Deng, C. Li, S. Chen, Q. Zhou, Z. Xu, Z. Wang, H. Yao, H. Hirao and G. Zhu, An intramolecular photoswitch can significantly promote photoactivation of Pt(IV) prodrugs, *Chem. Sci.*, 2021, **12**, 6536–6542.

103 D. Tolan, V. Gandin, L. Morrison, A. El-Nahas, C. Marzano, D. Montagner and A. Erxleben, Oxidative stress induced by Pt(IV) pro-drugs based on the cisplatin scaffold and indole carboxylic acids in axial position, *Sci. Rep.*, 2016, **6**, 29367.

104 H. Yao, Z. Xu, C. Li, M. K. Tse, Z. Tong and G. Zhu, Synthesis and cytotoxic study of a platinum(IV) anticancer prodrug with selectivity toward luteinizing hormone-releasing hormone (LHRH) receptor-positive cancer cells, *Inorg. Chem.*, 2019, **58**, 11076–11084.

105 H. Yao, Y. F. Gunawan, G. Liu, M.-K. Tse and G. Zhu, Optimization of axial ligands to promote the photoactivation of BODIPY-conjugated platinum(IV) anticancer prodrugs, *Dalton Trans.*, 2021, **50**, 13737–13747.

106 Z. Deng, N. Wang, Y. Liu, Z. Xu, Z. Wang, T.-C. Lau and G. Zhu, A photocaged, water-oxidizing, and nucleolus-targeted Pt(IV) complex with a distinct anticancer mechanism, *J. Am. Chem. Soc.*, 2020, **142**, 7803–7812.

107 G. R. Gibbons, S. Wyrick and S. G. Chaney, Rapid reduction of tetrachloro(D,L-*trans*)1,2-diaminocyclohexaneplatinum(IV) (tetraplatin) in RPMI 1640 tissue culture medium, *Cancer Res.*, 1989, **49**, 1402–1407.

108 W. K. Anderson, D. A. Quagliato, R. D. Haugwitz, V. L. Narayanan and M. K. Wolpert-DeFilippes, Synthesis, physical properties, and antitumor activity of tetraplatin and related tetrachloroplatinum(IV) stereoisomers of 1,2-diaminocyclohexane, *Cancer Treat. Rep.*, 1986, **70**, 997–1002.

109 S. G. Chaney, S. Wyrick and G. K. Till, *In vitro* biotransformations of tetrachloro(d,l-*trans*,)-1,2-diaminocyclohexaneplatinum(IV) (tetraplatin) in rat plasma, *Cancer Res.*, 1990, **50**, 4539–4545.

110 L. Pendyala, J. W. Cowens and P. J. Creaven, Studies on the pharmacokinetics and metabolism of *cis*-dichloro-*trans*-dihydroxy-bis-isopropylamine platinum(IV) in the dog, *Cancer Treat. Rep.*, 1982, **66**, 509–516.

111 D. J. Evans and M. Green, The rate of reduction of *cis*-, *cis*-, *trans*-$[PtIV(NH_2Pr^i)_2Cl_2(OH)_2]$, CHIP, the anti-cancer drug by ascorbic acid, *Inorg. Chim. Acta*, 1987, **130**, 183–184.

112 T. Babu, A. Sarkar, S. Karmakar, C. Schmidt and D. Gibson, Multiaction Pt(IV) carbamate complexes can codeliver Pt(II) drugs and amine containing bioactive molecules, *Inorg. Chem.*, 2020, **59**, 5182–5193.

113 S. Karmakar, H. Kostrhunova, T. Ctvrtlikova, V. Novohradsky, D. Gibson and V. Brabec, Platinum(IV)-estramustine multiaction prodrugs are effective antiproliferative agents against prostate cancer cells, *J. Med. Chem.*, 2020, **63**, 13861–13877.

114 Y. Song, K. Suntharalingam, J. S. Yeung, M. Royzen and S. J. Lippard, Synthesis and characterization of Pt(IV) fluorescein conjugates to investigate Pt(IV) intracellular transformations, *Bioconjugate Chem.*, 2013, **24**, 1733–1740.

115 H. Shi, Q. Wang, V. Venkatesh, G. Feng, L. S. Young, I. Romero-Canelón, M. Zeng and P. J. Sadler, Photoactive platinum(IV) complex conjugated to a cancer-cell-targeting cyclic peptide, *Dalton Trans.*, 2019, **48**, 8560–8564.

116 G. Liu, Y. Zhang, H. Yao, Z. Deng, S. Chen, Y. Wang, W. Peng, G. Sun, M.-K. Tse, X. Chen, J. Yue, Y. Peng, L. Wang and G. Zhu, An ultrasound-activatable platinum prodrug for sono-sensitized chemotherapy, *Sci. Adv.*, 2023, **9**, eadg5964.

117 H. Xiao, R. Qi, S. Liu, X. Hu, T. Duan, Y. Zheng, Y. Huang and X. Jing, Biodegradable polymer – cisplatin(IV) conjugate as a pro-drug of cisplatin(II), *Biomaterials*, 2011, **32**, 7732–7739.

118 S. Theiner, M. Grabarics, L. Galvez, H. P. Varbanov, N. S. Sommerfeld, M. S. Galanski, B. K. Keppler and G. Koellensperger, The impact of whole human blood on the kinetic inertness of platinum(IV) prodrugs – an HPLC-ICP-MS study, *Dalton Trans.*, 2018, **47**, 5252–5258.

119 L. T. Ellis, H. M. Er and T. W. Hambley, The influence of the axial ligands of a series of platinum(IV) anti-cancer complexes on their reduction to platinum(II) and reaction with DNA, *Aust. J. Chem.*, 1995, **48**, 793–806.

120 C. K. J. Chen, J. Z. Zhang, J. B. Aitken and T. W. Hambley, Influence of equatorial and axial carboxylato ligands on the kinetic inertness of platinum(IV) complexes in the presence of ascorbate and cysteine and within DLD-1 cancer cells, *J. Med. Chem.*, 2013, **56**, 8757–8764.

121 O. Proux, E. Lahera, W. Del Net, I. Kieffer, M. Rovezzi, D. Testemale, M. Irar, S. Thomas, A. Aguilar-Tapia and E. F. Bazarkina, High-energy resolution fluorescence detected X–ray absorption spectroscopy: a powerful new structural tool in environmental biogeochemistry sciences, *J. Environ. Qual.*, 2017, **46**, 1146–1157.

122 S. J. Berners-Price, L. Ronconi and P. J. Sadler, Insights into the mechanism of action of platinum anticancer drugs from multinuclear NMR spectroscopy, *Prog. Nucl. Magn. Reson. Spectrosc.*, 2006, **1**, 65–98.

123 E. E. Blatter, J. F. Vollano, B. S. Krishnan and J. C. Dabrowiak, Interaction of the antitumor agents *cis*,*cis*,*trans*-Pt(IV)$(NH_3)_2Cl_2(OH)_2$ and *cis*,*cis*,*trans*-Pt(IV)$[(CH_3)_2CHNH_2]_2Cl_2(OH)_2$ and their reduction products with PM2 DNA, *Biochemistry*, 1984, **23**, 4817–4820.

124 H. Yao, S. Chen, Z. Deng, M.-K. Tse, Y. Matsuda and G. Zhu, BODI-Pt, a green-light-activatable and carboplatin-based platinum(IV) anticancer prodrug with enhanced activation and cytotoxicity, *Inorg. Chem.*, 2020, **59**, 11823–11833.

125 E. Wexselblatt, R. Raveendran, S. Salameh, A. Friedman-Ezra, E. Yavin and D. Gibson, On the stability of Pt^{IV} pro–drugs with haloacetato ligands in the axial positions, *Chem. – Eur. J.*, 2015, **21**, 3108–3114.

126 S. J. Berners-Price, L. Ronconi and P. J. Sadler, Insights into the mechanism of action of platinum anticancer drugs from multinuclear NMR spectroscopy, *Prog. Nucl. Magn. Reson. Spectrosc.*, 2006, **49**, 65–98.

127 C. K. J. Chen, P. Kappen, D. Gibson and T. W. Hambley, *trans*-Platinum(IV) pro-drugs that exhibit unusual resistance to reduction by endogenous reductants and blood serum but are rapidly activated inside cells: ^{1}H NMR and XANES spectroscopy study, *Dalton Trans.*, 2020, **49**, 7722–7736.

128 L. Chen, P. F. Lee, J. D. Ranford, J. J. Vittal and S. Y. Wong, Reduction of the anti-cancer drug analogue *cis*,*trans*,*cis*-$[PtCl_2(OCOCH_3)_2(NH_3)_2]$ by L-cysteine and L-methionine and its crystal structure, *Dalton Trans.*, 1999, 1209–1212.

129 V. E. Y. Lee, C. F. Chin and W. H. Ang, Design and investigation of photoactivatable platinum(IV) prodrug complexes of cisplatin, *Dalton Trans.*, 2019, **48**, 7388–7393.

130 J. Gurruchaga-Pereda, V. Martínez-Martínez, E. Rezabal, X. Lopez, C. Garino, F. Mancin, A. L. Cortajarena and L. Salassa, Flavin bioorthogonal photocatalysis toward platinum substrates, *ACS Catal.*, 2020, **10**, 187–196.

131 M. Sinisi, F. P. Intini and G. Natile, Dependence of the reduction products of platinum(IV) prodrugs upon the configuration of the substrate, bulk of the carrier ligands, and nature of the reducing agent, *Inorg. Chem.*, 2012, **51**, 9694–9704.

132 T. G. Appleton, R. D. Berry, C. A. Davis, J. R. Hall and H. A. Kimlin, Reactions of platinum(II) aqua complexes. 1. Multinuclear (platinum-195, nitrogen-15, and phosphorus-31) NMR study of reactions between the *cis*-diamminediaquaplatinum(II) cation and the oxygen-donor ligands hydroxide, perchlorate, nitrate, sulfate, phosphate, and acetate, *Inorg. Chem.*, 1984, **23**, 3514–3521.

133 T. G. Appleton, J. R. Hall and S. F. Ralph, Reactions of platinum(II) aqua complexes. 3. Multinuclear (nitrogen-15, platinum-195, carbon-13, and proton) NMR study of reactions of aqua and hydroxo complexes with glycine and (methylimino)diacetic acid, *Inorg. Chem.*, 1985, **24**, 673–677.

134 D. Corinti, M. E. Crestoni, S. Fornarini, E. Dabbish, E. Sicilia, E. Gabano, E. Perin and D. Osella, A multi-methodological inquiry of the behavior of cisplatin-based Pt(IV) derivatives in the presence of bioreductants with a focus on the isolated encounter complexes, *J. Biol. Inorg. Chem.*, 2020, **25**, 655–670.

135 L. Ronconi and P. J. Sadler, Photoreaction pathways for the anticancer complex *trans*,*trans*,*trans*-$[Pt(N_3)_2(OH)_2(NH_3)_2]$, *Dalton Trans.*, 2011, **40**, 262–268.

136 A. Nemirovski, Y. Kasherman, Y. Tzaraf and D. Gibson, Reduction of *cis*,*trans*,*cis*-$[PtCl_2(OCOCH_3)_2(NH_3)_2]$ by

aqueous extracts of cancer cells, *J. Med. Chem.*, 2007, **50**, 5554–5556.

137 A. Lasorsa, O. Stuchlíková, V. Brabec, G. Natile and F. Arnesano, Activation of platinum(IV) prodrugs by cytochrome *c* and characterization of the protein binding sites, *Mol. Pharmaceutics*, 2016, **13**, 3216–3223.

138 M. Ravera, E. Gabano, S. Tinello, I. Zanellato and D. Osella, May glutamine addiction drive the delivery of antitumor cisplatin-based Pt(IV) prodrugs?, *J. Inorg. Biochem.*, 2017, **167**, 27–35.

139 N. Kratochwil, P. J. Bednarski, H. Mrozek, A. Vogler and J. K. Nagle, Photolysis of an iodoplatinum(IV) diamine complex to cytotoxic species by visible light, *Anti-Cancer Drug Des.*, 1996, **11**, 155–171.

140 N. A. Kratochwil, Z. Guo, P. S. Murdoch, J. A. Parkinson, P. J. Bednarski and P. J. Sadler, Electron-transfer-driven trans-ligand labilization: a novel activation mechanism for Pt(IV) anticancer complexes, *J. Am. Chem. Soc.*, 1998, **120**, 8253–8254.

141 N. A. Kratochwil, J. A. Parkinson, P. J. Bednarski and P. J. Sadler, Nucleotide platination induced by visible light, *Angew. Chem., Int. Ed.*, 1999, **38**, 1460–1463.

142 P. Müller, B. Schröder, J. A. Parkinson, N. A. Kratochwil, R. A. Coxall, A. Parkin, S. Parsons and P. J. Sadler, Nucleotide cross–linking induced by photoreactions of platinum(IV)–azide complexes, *Angew. Chem., Int. Ed.*, 2003, **42**, 335–339.

143 P. J. Bednarski, R. Grünert, M. Zielzki, A. Wellner, F. S. Mackay and P. J. Sadler, Light-activated destruction of cancer cell nuclei by platinum diazide complexes, *Chem. Biol.*, 2006, **13**, 61–67.

144 F. S. Mackay, J. A. Woods, P. Heringová, J. Kašpárková, A. M. Pizarro, S. A. Moggach, S. Parsons, V. Brabec and P. J. Sadler, A potent cytotoxic photoactivated platinum complex, *Proc. Natl. Acad. Sci. U. S. A.*, 2007, **104**, 20743–20748.

145 P. Lepucki, A. P. Dioguardi, D. Karnaushenko, O. G. Schmidt and H.-J. Grafe, The normalized limit of detection in NMR spectroscopy, *J. Magn. Reson.*, 2021, **332**, 107077.

146 E. P. Diamandis, Immunoassays with time-resolved fluorescence spectroscopy: principles and applications, *Clin. Biochem.*, 1988, **21**, 139–150.

147 J. Bridgeman, M. Bieroza and A. Baker, The application of fluorescence spectroscopy to organic matter characterisation in drinking water treatment, *Rev. Environ. Sci. Biotechnol.*, 2011, **10**, 277–290.

148 O. S. Wolfbeis, *Fluorescence spectroscopy: new methods and applications*, Springer Science & Business Media, 2012.

149 X. Jiang, Y. Yu, J. Chen, M. Zhao, H. Chen, X. Song, A. J. Matzuk, S. L. Carroll, X. Tan, A. Sizovs, N. Cheng, M. C. Wang and J. Wang, Quantitative imaging of glutathione in live cells using a reversible reaction-based ratiometric fluorescent probe, *ACS Chem. Biol.*, 2015, **10**, 864–874.

150 K. Umezawa, M. Yoshida, M. Kamiya, T. Yamasoba and Y. Urano, Rational design of reversible fluorescent probes for live-cell imaging and quantification of fast glutathione dynamics, *Nat. Chem.*, 2017, **9**, 279–286.

151 H. Liu, W. Song, S. Zhang, K. S. Chan, Z. Guo and Z. Shen, A ratiometric fluorescent probe for real-time monitoring of intracellular glutathione fluctuations in response to cisplatin, *Chem. Sci.*, 2020, **11**, 8495–8501.

152 E. J. New, R. Duan, J. Z. Zhang and T. W. Hambley, Investigations using fluorescent ligands to monitor platinum(IV) reduction and platinum(II) reactions in cancer cells, *Dalton Trans.*, 2009, 3092–3101.

153 Y. Yuan, Y. Chen, B. Z. Tang and B. Liu, A targeted theranostic platinum(IV) prodrug containing a luminogen with aggregation-induced emission (AIE) characteristics for *in situ* monitoring of drug activation, *Chem. Commun.*, 2014, **50**, 3868–3870.

154 C. Shen, B. D. W. Harris, L. J. Dawson, K. A. Charles, T. W. Hambley and E. J. New, Fluorescent sensing of monofunctional platinum species, *Chem. Commun.*, 2015, **51**, 6312–6314.

155 C. S. Wijesooriya, J. A. Peterson, P. Shrestha, E. J. Gehrmann, A. H. Winter and E. A. Smith, A photoactivatable BODIPY probe for localization–based super–resolution cellular imaging, *Angew. Chem., Int. Ed.*, 2018, **57**, 12685–12689.

156 M. H. C. Boulet, H. R. Bolland, E. M. Hammond and A. C. Sedgwick, Oxali(IV)Fluors: fluorescence responsive oxaliplatin(IV) complexes identify a hypoxia-dependent reduction in cancer cells, *J. Am. Chem. Soc.*, 2023, **145**, 12998–13002.

157 Y. Yuan, R. T. K. Kwok, B. Z. Tang and B. Liu, Targeted theranostic platinum(IV) prodrug with a built-in aggregation-induced emission light-up apoptosis sensor for non-invasive early evaluation of its therapeutic responses in situ, *J. Am. Chem. Soc.*, 2014, **136**, 2546–2554.

158 J. J. Wilson and S. J. Lippard, Modulation of ligand fluorescence by the Pt(II)/Pt(IV) redox couple, *Inorg. Chim. Acta*, 2012, **389**, 77–84.

159 C. Boudreau, T.-L. Wee, Y.-R. Duh, M. P. Couto, K. H. Ardakani and C. M. Brown, Excitation light dose engineering to reduce photo-bleaching and photo-toxicity, *Sci. Rep.*, 2016, **6**, 30892.

160 P. M. Carlton, J. Boulanger, C. Kervrann, J.-B. Sibarita, J. Salamero, S. Gordon-Messer, D. Bressan, J. E. Haber, S. Haase, L. Shao, L. Winoto, A. Matsuda, P. Kner, S. Uzawa, M. Gustafsson, Z. Kam, D. A. Agard and J. W. Sedat, Fast live simultaneous multiwavelength four-dimensional optical microscopy, *Proc. Natl. Acad. Sci. U. S. A.*, 2010, **107**, 16016–16022.

161 S. Wäldchen, J. Lehmann, T. Klein, S. Van De Linde and M. Sauer, Light-induced cell damage in live-cell super-resolution microscopy, *Sci. Rep.*, 2015, **5**, 15348.

